# The Dynamical Evolution of Young Clusters

## With a focus on the effects on planetary systems

*Clément Bonnerot*

Lund Observatory
Lund University

2011-EXA55

Degree project of 15 higher education credits
August 2011

Lund Observatory
Box 43
SE-221 00 Lund
Sweden

**Abstract**

Stars form in clusters or groups. In these crowded environments, they are likely to experience encounters with one another. These encounters may perturb their planetary systems and cause the ejection of one or more planets. N-body simulations were performed to study the effect of encounters between stars on their planetary systems in young stellar clusters. Two categories of young clusters were modelled : clusters without gas (dry clusters) and clusters containing gas (embedded clusters). In both cases, it was found that a large majority of stars (85 - 95 %) experience at least one encounter with an other star in the first 10 Myr of the cluster evolution. Furthermore, between 5 % and 25 % of solar system-like planetary systems are affected by these encounters.

# Acknowledgements

I would like to thank Melvyn B. Davies for giving me the opportunity to work on this interesting subject. He helped me to adopt a scientific method throughout my internship. By discussing with him, I was able to take a critical look at my work which allowed me to better understand my results. He also made me aware of the big picture of my project. I also want to thank Ross Church for his careful explanations about both technical subjects like FORTRAN programming and scientific ones like cluster dynamics. I highly appreciated the patience he showed while doing it.

I also thank all the people of the Astronomy department for creating a pleasant environment to work and learn. They immediately made me feel comfortable in the observatory. In particular, I appreciated the animated daily coffee breaks. I also learnt a lot from the seminars, NOTA and OTA meetings and Journal Club. They allowed me to discover numerous interesting topics related to astronomy.

# Contents

**1 Introduction** **6**

**2 Early cluster environment** **6**
2.1 Effect of the gaseous component . . . . . 6
2.2 Gas expulsion . . . . . 7

**3 Impact on planetary systems** **9**
3.1 Fly-bys . . . . . 10
3.2 Exchange encounters . . . . . 11

**4 N-body simulations performed** **12**
4.1 Dry clusters (without gas) . . . . . 12
4.2 Embedded clusters (with gas) . . . . . 16

**5 Results** **17**
5.1 Dry clusters (without gas) . . . . . 17
5.1.1 Clusters evolution . . . . . 17
5.1.2 Rate and closest approaches of fly-bys . . . . . 20
5.1.3 Binaries properties . . . . . 24
5.1.4 Impact on planetary systems . . . . . 25
5.1.5 Influence of initial positions . . . . . 27
5.2 Embedded clusters (with gas) . . . . . 29
5.2.1 Clusters evolution . . . . . 29
5.2.2 Rate and closest approaches of fly-bys . . . . . 32
5.2.3 Binaries properties . . . . . 35
5.2.4 Impact on planetary systems . . . . . 36

**6 Discussion** **38**
6.1 Post-encounters evolution of planetary systems . . . . . 38
6.2 Impact of fly-bys on wide planets . . . . . 43
6.3 Effect of mass segregation . . . . . 44

**7 Conclusion** **47**

# 1 Introduction

According to observational data, most of the stars (70 - 90 %) form in clusters (Lada and Lada, 2003). These structures contain from a few tens to a few thousand stars. In these dense regions, stars are likely to undergo encounters with one another. These encounters are mainly of two sorts : fly-bys – two stars passing close to each other – and exchange encounters – a star replacing one of the two components of an existing binary. Both can affect planetary systems by perturbing the orbits of the planets.

Furthermore, the clusters are initially embedded in giant molecular clouds (GMCs). This gas is responsible for an additional gravitational potential. Therefore it has a influence on the clusters dynamics. This gas is expelled $\sim$ 10 Myr after the end of the stellar formation. It induces an expansion of the cluster which can cause it to unbind in $\sim$ 10 Myr. This evolution of young stellar clusters has an influence on the properties of encounters between stars and therefore determines how their planetary systems are perturbed.

The main goal of this project is to investigate how planetary systems are affected in these clusters via N-body simulations. In particular, an important number to evaluate is the number of singletons i.e. the number of stars which never experience any encounter during the cluster evolution. Indeed, a star which is not a singleton may have its planets' orbits perturbed by the effects of these encounters. Hence this number allows to estimate how rare unaffected planetary systems are.

This report is arranged as follows. In section 2, the early cluster environment is described. In particular, the effects of the gas and its subsequent expulsion are pointed out. Section 3 depicts the different sorts of encounters between stars which occur in stellar clusters. Their effects on planetary systems are also studied. In section 4, the N-body simulations performed are described. The results of these simulations are presented in section 5. The clusters' evolution is presented first. Then its effect on encounter properties and planetary systems is assessed. In section 6, these simulations are used to discuss the post-encounter evolution, the impact of fly-bys on wide planets and the effect of mass segregation.

# 2 Early cluster environment

## 2.1 Effect of the gaseous component

A significant fraction of stars is born embedded within the densest regions of GMCs. After this star formation period, which last $\sim$ 1 Myr, a certain amount of gas is left-over. The fraction of gas remaining depends on the star formation efficiency (SFE) of the cluster, i.e. the fraction of the initial mass of gas which has been spent to form stars. Thus a high SFE corresponds to a low mass of gas remaining although a low SFE implies that a high mass of gas remains after the star formation process.

This gas has an influence on the dynamics of embedded clusters through an additional term in the gravitational potential. The potential energy $\Omega_{\rm emb}$ of an embedded cluster

is given by

$$\Omega_{\rm emb} = \Omega_\star + \Omega_{\rm gas} \tag{1}$$

where $\Omega_\star$ and $\Omega_{\rm gas}$ are the potential energy due to the stars and the gas. The cluster evolves to reach virial equilibrium. When this equilibrium is achieved, kinetic and potential energies of the cluster $T_{\rm emb}$ and $\Omega_{\rm emb}$ are related by

$$T_{\rm emb} = -\frac{1}{2}\Omega_{\rm emb}. \tag{2}$$

Their so-called virial ratio defined by $Q_{\rm emb} = |T_{\rm emb}/\Omega_{\rm emb}|$ is then equal to 0.5. As the kinetic energy of the cluster is equal to that of its stars $T_\star$, it yields

$$\left|\frac{T_\star}{\Omega_\star + \Omega_{\rm gas}}\right| = 0.5. \tag{3}$$

Assuming that the stars are initially in virial equilibrium with $|T_\star/\Omega_\star| = 0.5$, the condition given by equation 3 in not verified. It means that the cluster is not in virial equilibrium initially. Indeed, initial velocities of the stars are not high enough to resist the central attraction of the cluster (due to the gas and the stars). Hence, they will sink to the centre of the cluster.

A dynamically similar situation exists for a cluster without gas, called dry in the following. The potential and kinetic energies of this cluster are reduced to those of its stars. Hence, virial equilibrium of this cluster is given by

$$\left|\frac{T_\star}{\Omega_\star}\right| = 0.5. \tag{4}$$

Assuming that the stars are initially not in virial equilibrium with $|T_\star/\Omega_\star| < 0.5$, the subsequent evolution of these stars will be similar to the previous one in an embedded cluster. Indeed, their initial velocities are lower than virial ones and they will sink to the centre of the cluster to reach the equilibrium of equation 4. In addition to embedded clusters, this equivalent situation will be studied by N-body simulations in section 4.

## 2.2 Gas expulsion

Several mechanisms such as UV emissions, strong stellar winds and supernovae are energetic enough ($\sim 10^{51}$ erg) to expel the remaining gas from the cluster (Goodwin, 1997). One can show it by comparing the energy of these mechanisms to the binding energy of the gas in the cluster. As it will be assumed in section 4, the gas can be modelled by a Plummer density distribution. It is defined by equation 37. From this formula, I calculated the binding energy of the gas in the cluster using

$$E_{\rm bind} = -\int_{r=0}^{\infty} \frac{Gm(r){\rm d}m}{r}. \tag{5}$$

where $m(r)$ is the mass of the gas contained within a radius r in the cluster. The calculation yielded

$$E_{\rm bind} = -K\frac{Gm_{\rm gas}^2}{r_h} \tag{6}$$

where $m_{\rm gas}$ is the total mass of the gas in the cluster and $K = \frac{9\pi}{256\,1.305} \simeq 0.08$. For the clusters modelled in the following, $m_{\rm gas} = 425\,{\rm M}_\odot$ and $r_{\rm h} = 0.38\,{\rm pc}$ which yields $E_{\rm bind} \simeq 3 \times 10^{45}\,{\rm erg}$. Therefore $-E_{\rm bind} < 10^{51}\,{\rm erg}$ and the gas can indeed be expelled from the cluster by the previous mechanisms.

This removal happens at $\sim 10$ Myr after the end of the stellar formation. The gravitational potential of the cluster is then reduced to that of the stars. The timescale of this removal is not well defined, it varies with the predominant removal mechanism. Owing to the decrease of the potential, the escape velocity falls off thus enabling the escape of initially bound stars from the cluster. The cluster can then unbind or find another virial equilibrium after a period of violent relaxation (Goodwin and Bastian, 2006). The destiny of the cluster is mainly determined by its SFE and the timescale of the gas removal. The influence of these two parameters will now be studied.

The effect of the gas removal timescale is described first. As a first approach, a similar problem will be studied : the effect of mass loss with two different timescales from a star on a planet orbiting it. The mass loss will be first considered instantaneous. Then it will be assumed to occur very slowly. Let first consider that the host star looses half of its mass instantaneously. Before this mass loss, the velocity of the planet is given by

$$v_i = \sqrt{\frac{G m_{\rm s}}{R}} \tag{7}$$

where $m_{\rm s}$ is the mass of the star and $R$ the distance between the star and the planet. On the other hand, the escape velocity of the planet at that time is given by

$$\left(v_{\rm esc}\right)_i = \sqrt{\frac{2\,G m_{\rm s}}{R}}. \tag{8}$$

As $v_i = \frac{(v_{\rm esc})_i}{\sqrt{2}} < \left(v_{\rm esc}\right)_i$, the planet is initially bound to the star. After the mass loss, the velocity of the planet $v_f$ is equal to the initial one $v_i$ because it occurs instantaneously :

$$v_f = v_i = \sqrt{\frac{G m_{\rm s}}{R}}. \tag{9}$$

However, the mass loss from the host star induces a decrease of the escape velocity. When the star has lost half of its mass, it is then given by

$$\left(v_{\rm esc}\right)_f = \sqrt{\frac{G m_{\rm s}}{R}}. \tag{10}$$

As $v_f = \left(v_{\rm esc}\right)_f$, the planet escapes from the star. Let now assume that the star looses half of its mass very slowly. This mass loss will not lead to an escape of the planet. Instead, the orbit of the planet will double. Hence, the mass loss timescale affects a lot the subsequent evolution of the system. It turns out that the effect of the mass loss timescale on a planetary system is similar to that of the gas removal timescale on a cluster. A rapid gas removal compared to the dynamical timescale of the cluster is likely to unbind it. In contrast, a very slow one will simply lead to an expansion of the cluster.

The effect of the SFE is know studied. A borderline case, known as the Hills' problem (Hills, 1980), consists to consider the gas removal instantaneous and the stars to be initially in virial equilibrium. This problem is studied by Boily and Kroupa (2003). The assumption of initial virial equilibrium allows to calculate the initial velocity dispersion of the stars by

$$\overline{v^2}_0 = \frac{GM_0}{R_0} \tag{11}$$

where $M_0 = M_\star + M_{\rm gas}$ is the initial mass of the cluster and $R_0$ its initial radius. As the gas removal occurs instantaneously, the velocity dispersion after this removal is equal to the initial one : $\overline{v^2} = \overline{v^2}_0$. The cluster has a mass $M_\star$ and a radius $R_0$. Hence its binding energy just after the removal is given by

$$E = \frac{1}{2} M_\star \overline{v^2}_0 - \frac{G{M_\star}^2}{R_0}. \tag{12}$$

Afterwards, the cluster expands and finds another virial equilibrium with a radius $R$. When this equilibrium is reached, its binding energy is

$$E = -\frac{1}{2}\frac{G{M_\star}^2}{R}. \tag{13}$$

Combining equations 11, 12 and 13, it yields

$$\frac{R}{R_0} = \frac{M_\star}{M_\star - M_{\rm gas}}. \tag{14}$$

One can see that $R \longrightarrow \infty$ for $M_{\rm gas} = M_\star$. Hence, the condition for the cluster to stay bound is given by

$$M_{\rm gas} < M_\star. \tag{15}$$

In other words, it stays bound if less than 50 % of the initial mass is composed of gas which corresponds to a SFE of 0.5 if the gas removal is instantaneous.

Therefore, the combined effects of the SFE and the removal timescale can be summarized as follows. If the gas removal is rapid, i.e. its timescale can be neglected compared to the dynamical timescale of the cluster, it unbinds the cluster if its SFE is equal to or lower than 0.5. However, if the gas removal is slow, the cluster can resist it even for SFE lower than 0.5. Instead of destroying it, the gas removal causes the cluster to expand by a factor which depends on its SFE.

# 3 Impact on planetary systems

Stellar clusters are dangerous places for planetary systems. Indeed, most of the stars will undergo encounters with other stars of the cluster which are likely to perturb their planetary systems. These encounters can be divided into two categories : fly-bys and exchange encounters with a binary. They will be studied in the two next sections.

## 3.1 Fly-bys

Fly-bys occur when two stars of the cluster pass close – typically with a minimum distance lower than 1000 AU – to each other. When a star undergoes a fly-by, the orbits of its planets are perturbed. This perturbation may cause an immediate ejection of one or more planet due to planet-planet scattering. They can also be followed by a long phase of planet-planet interactions which can eventually lead to a late ejection of one or more planets. The post-fly-bys evolution of planetary systems will be considered in section 6.1.

The effect of an incoming star on a planetary system depends on its kinetic energy. Due to the conservation of energy before and after the fly-by, the incoming star will unbind the planetary system if its kinetic energy is greater than the binding energy of the planetary system. Applied to a planetary system composed of one planet, this condition is

$$\frac{1}{2} m_{\mathrm{i}} {v_{\mathrm{i}}}^2 > \frac{G m_{\mathrm{h}} m_{\mathrm{p}}}{2a} \tag{16}$$

where $m_{\mathrm{i}}$ and $v_{\mathrm{i}}$ are the mass and the velocity of the incoming star, $m_{\mathrm{h}}$ and $m_{\mathrm{p}}$ are the masses of the host star and the planet and $a$ is the semi-major axis of the planet. As a consequence, wide planets are more likely to be unbound because their binding energy is lower. The effects of fly-bys on these sorts of planets will be studied in section 6.2.

Moreover, the effects of fly-bys also depend on their minimum distance of approach. Close fly-bys can cause the ejection of one or more planets. In contrast, most of wide fly-bys just slightly disturb the orbit of the outermost planet of the system. The cross-section $\sigma$ for two stars to pass within a minimum distance $r_{\mathrm{min}}$ can be determined analytically (Armitage, 2010). It is given by

$$\sigma = \pi r_{\mathrm{min}}^2 \left(1 + \frac{v^2}{v_\infty^2}\right) \tag{17}$$

where $v_\infty$ is the relative velocity at infinity of the two stars. $v$ is the relative velocity of the two stars at closest approach for a parabolic encounter. It is given by

$$v^2 = \frac{2G(m_1 + m_2)}{r_{\mathrm{min}}}. \tag{18}$$

The second term in brackets in equation 17 induces an increase of $\sigma$. It is due to the deflection of the trajectories due to the gravitational attraction. This mechanism is called gravitational focussing. Two regimes have now to be considered depending on the velocity dispersion. In the first one, $v_\infty \ll v$, which is the case for young clusters with low velocity dispersion. $\sigma$ is then proportional to $r_{\mathrm{min}}$ according to equations 17 and 18 :

$$\sigma \propto r_{\mathrm{min}}. \tag{19}$$

In the second regime, $v_\infty \gg v$. In this case, $\sigma$ is proportional to $r_{\mathrm{min}}^2$ :

$$\sigma \propto r_{\mathrm{min}}^2. \tag{20}$$

The timescale for a given star to undergo an encounter in a young cluster (where $v_\infty \ll v$) can be derived from equation 19. It is given by

$$\tau_{\rm enc} \simeq 3.3 \times 10^7\,{\rm yr} \left(\frac{100\,{\rm pc}^{-3}}{n}\right)\left(\frac{v_\infty}{1\,{\rm km\,s}^{-1}}\right)\left(\frac{10^3\,{\rm AU}}{r_{\rm min}}\right)\left(\frac{{\rm M}_\odot}{m_{\rm t}}\right) \tag{21}$$

where $n$ is the stellar number density in the cluster, $v_\infty$ the mean relative speed at infinity of the objects in the cluster, $r_{\rm min}$ the encounter distance and $m_{\rm t}$ the total mass of the objects involved in the encounter (Binney and Tremaine, 1987). From the previous formula, Malmberg et al. (2007b) derived one which is more adapted to stellar clusters. It is given by

$$\tau_{\rm enc} \simeq 5 \times 10^7\,{\rm yr} \left(\frac{\bar{m}_*}{{\rm M}_\odot}\right)\left(\frac{r_{\rm h}}{1\,{\rm pc}}\right)^{5/2}\left(\frac{100\,{\rm M}_\odot}{m_{\rm cl}}\right)^{1/2}\left(\frac{10^3\,{\rm AU}}{r_{\rm min}}\right)\left(\frac{{\rm M}_\odot}{m_{\rm t}}\right) \tag{22}$$

where $\bar{m}_*$ is the mean mass of the stars, $r_{\rm h}$ the half-mass radius of the cluster, $m_{\rm cl}$ the mass of the cluster, $r_{\rm min}$ the encounter distance and $m_{\rm t}$ the total mass of the objects involved in the encounter. One can calculate this timescale for a typical cluster. For the clusters modelled in the following, it is assumed that $r_{\rm h} = 0.38\,{\rm pc}$ and $m_{\rm cl} = 425\,{\rm M}_\odot$ initially. Given the mass distributions for these clusters, the two other parameters can be taken to be $\bar{m}_* = 0.6\,{\rm M}_\odot$ and $m_{\rm t} = 1\,{\rm M}_\odot$. The encounter timescale for these clusters is then $\tau_{\rm enc} = 1.3\,{\rm Myr}$. This time is lower than the lifetime of these clusters. Hence, stars are likely to experience several encounters during the cluster lifetime.

## 3.2 Exchange encounters

Exchange encounters occur after a three-body interaction between an incoming single star and a binary where the incoming star replaces one of the components of the binary. However, the incoming star can also break up the binary. A binary which is broken up by an encounter with a third star, whose kinetic energy is equal to the average kinetic energy of the stars in the cluster, is termed soft. Otherwise, it is termed hard. Hard binaries are tighter than soft ones and therefore more bound. It allows to define a critical semi-major axis for binaries called the hard-soft boundary. When a single star encounters a hard binary, the latter is not broken up. Instead, if the mass of the incoming star exceeds that of one of the components of the binary, an exchange encounter can occur where the incoming star replaces the least massive star in the binary. A binary is broken up by an incoming star if its binding energy is lower than the kinetic energy of the star as seen preciously for a planetary system experiencing a fly-by. Hence, the condition for a binary to be hard in a cluster is given by

$$\frac{1}{2} m_{\rm i} v_\infty^2 < \frac{G m_1 m_2}{2a} \tag{23}$$

where $v_\infty$ is the velocity dispersion in the cluster, $m_{\rm i}$ is the mass of the incoming star, $m_1$ and $m_2$ are the masses of the binary components and $a$ is the semi-major axis. For a cluster containing $N$ stars, the hard-soft boundary can be approximated using equation 23 by assuming that all the stars in the cluster have the same mass. It yields :

$$a_{\rm hard-soft} \simeq \frac{r_{\rm h}}{N} \tag{24}$$

where $r_h$ is the half-mass radius (Malmberg et al., 2007b). For the clusters modelled in the following, $r_{\rm h} = 0.38\,{\rm pc}$ and $N = 700$ initially. Hence, an approximation of the hard-soft boundary is $a_{\rm hard-soft} \simeq 100{\rm AU}$.

A planetary system whose host star exchanges in a binary can be affected by the Kozai mechanism (Kozai, 1962). It occurs if the binary orbit is sufficiently inclined with respect to that of the planets. The critical inclination is given by

$$i_{\rm crit} = \cos^{-1}(\sqrt{\frac{3}{5}}) \simeq 39.2^{\circ}. \tag{25}$$

If this condition is verified, the Kozai mechanism leads to cyclical changes in the eccentricities of the planets with a maximum value of

$$e_{\rm max} = \sqrt{1 - \frac{5}{3}\cos^2(i)}. \tag{26}$$

This change in the eccentricities can cause orbits to cross and lead to the ejection of one or more planets. Malmberg et al. (2007a) found that this mechanism occurs in 77 % of the binaries formed by an exchange encounter. The evolution of planetary systems whose host star experience an exchange encounter will be considered in section 6.1.

# 4 N-body simulations performed

N-body simulations using a modified version of Sverre Aarseth's NBODY6 code (Aarseth, 1999) are performed to model the evolution of young stellar clusters. Dry clusters, i.e. clusters without gas, are modelled for five values of their initial virial ratio. The virial ratio is defined by the ratio of the kinetic energy of the cluster to its potential energy. Embedded clusters, i.e. clusters containing gas, are simulated for three different initial masses of gas.

## 4.1 Dry clusters (without gas)

The clusters studied contain 700 stars and has an initial half-mass radius of 0.38 pc which corresponds to one of the clusters modelled by Malmberg et al. (2007b). Simulations were performed for five values of the initial virial ratio Q : 0.5, 0.25, 0.1, 0.01 and 0.001. For each initial virial ratio, 25 realizations were carried out.

Initial positions of the stars follow the spherically symmetric Plummer distribution (Plummer, 1911) which is widely used to model clusters because of its simplicity. The density distribution, mass distribution and the associated potential are given by

$$\rho(r) = \frac{3m_{\rm cl}}{4\pi {r_0}^3}\left(1 + \frac{r^2}{r_0^2}\right)^{-5/2} \tag{27}$$

$$m(r) = m_{\rm cl}\left(1 + \frac{r_0^2}{r^2}\right)^{-3/2} \tag{28}$$

$$\Phi(r) = -\frac{G m_{\rm cl}}{r_0}\left(1+\frac{r^2}{r_0^2}\right)^{-1/2} \tag{29}$$

where $m_{\rm cl}$ is the mass of the cluster and $r_0$ a scaling factor which can be related to the half-mass radius $r_{\rm h}$ by $r_{\rm h} \simeq 1.305\, r_0$ (Heggie and Hut, 2003). I plot the density and mass profiles in figures 1 and 2 using the previous analytical formulae for $r_h = 0.38\,$pc and $m_{\rm cl} = 425\, M_\odot$. These values correspond to the modelled cluster. For the 25 realizations, different initial positions and velocities of the stars are used.

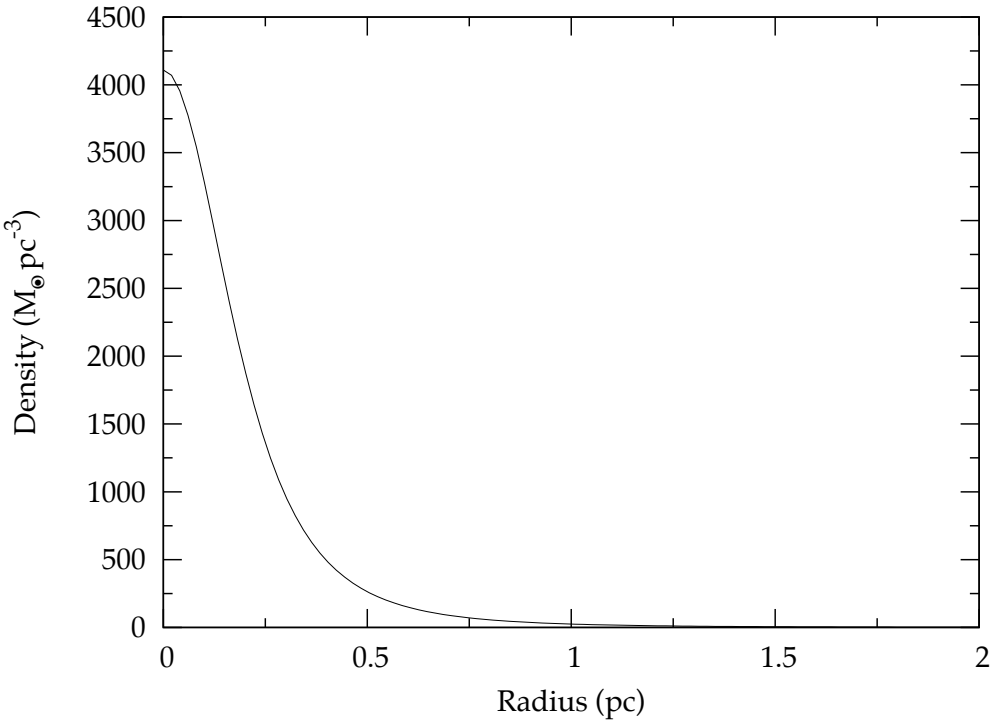


Figure 1: Density profile in a Plummer distribution with $r_h = 0.38\,$pc and $m_{\rm cl} = 425\, M_\odot$.

The masses of the stars range from 0.2 $\mathrm{M}_\odot$ to 5 $\mathrm{M}_\odot$. They follow the initial mass function (IMF) of Kroupa et al. (1993). The number of stars $\mathrm{d}N(M)$ whose masses are between $M$ and $M + \mathrm{d}M$ is then given by

$$\mathrm{d}N(M) = \xi(M)\,\mathrm{d}M \tag{30}$$

where

$$\xi(M) = \begin{cases} 0.035\, M^{-1.3} & \text{for} \quad 0.08\,\mathrm{M}_\odot \leq M < 0.5\,\mathrm{M}_\odot \\ 0.019\, M^{-2.2} & \text{for} \quad 0.5\,\mathrm{M}_\odot \leq M < 1.0\,\mathrm{M}_\odot \\ 0.019\, M^{-2.7} & \text{for} \quad M \geq 1.0\,\mathrm{M}_\odot \end{cases} \tag{31}$$

The masses of binary components are drawn independently from the IMF. I derived the cumulative number of stars as a function of the mass from the IMF for the modelled cluster which contains 700 stars with masses ranging from 0.2 $\mathrm{M}_\odot$ to 5 $\mathrm{M}_\odot$. I plot this distribution in figure 3. For the 25 realizations performed, different samples of stellar masses from the same distribution are used.

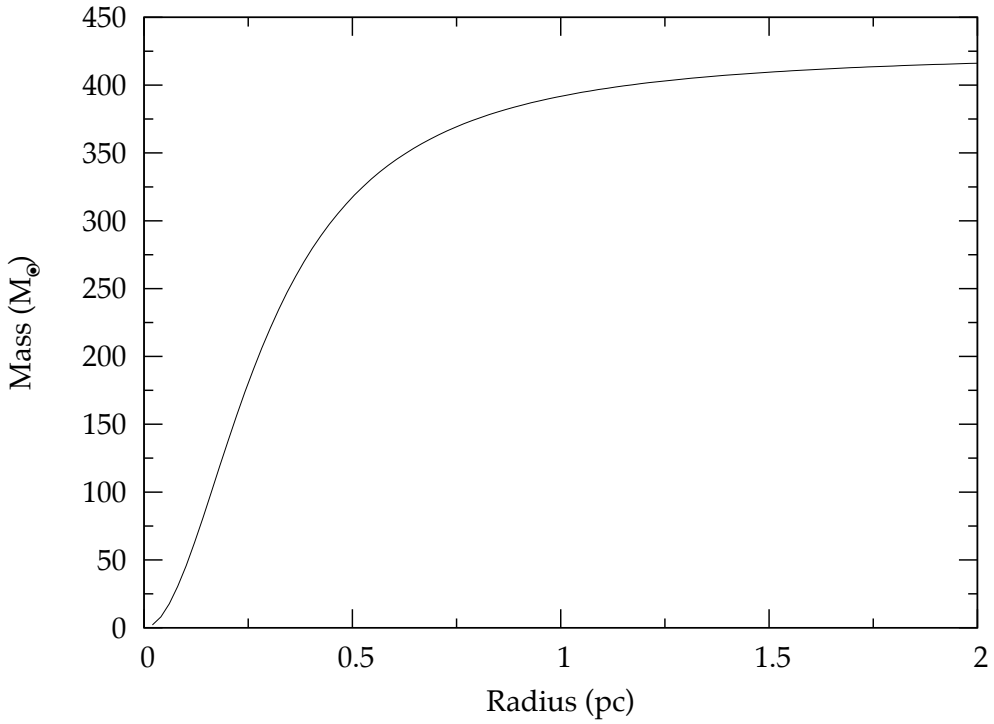


Figure 2: Mass profile in a Plummer distribution with $r_h = 0.38\,\mathrm{pc}$ and $m_{\mathrm{cl}} = 425\,M_\odot$.

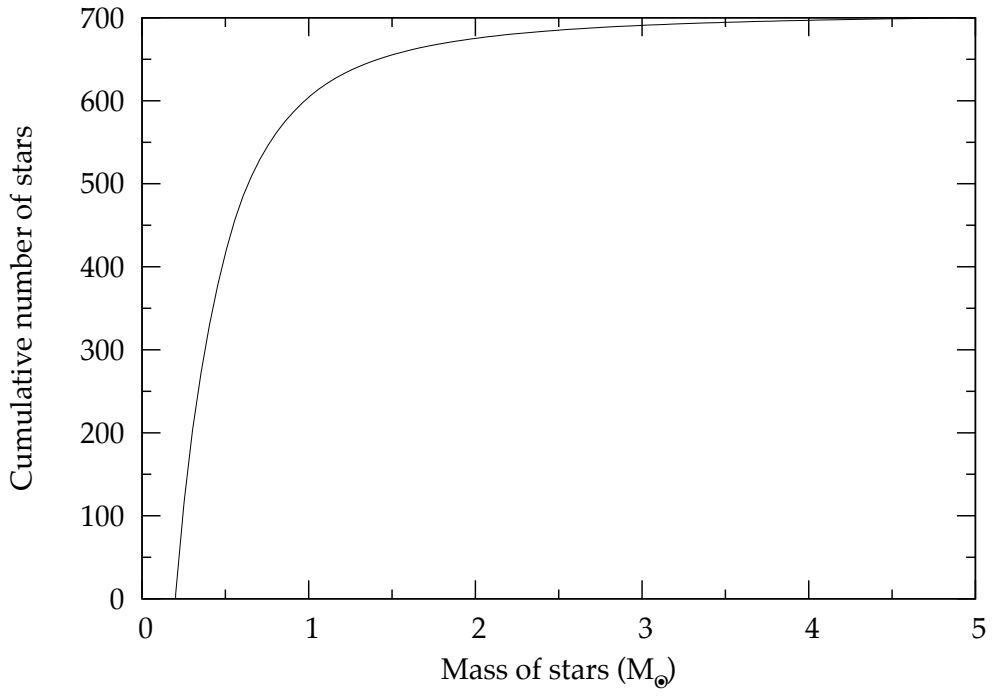


Figure 3: Kroupa IMF for a cluster containing 700 stars with masses ranging from 0.2 $M_\odot$ to 5 $M_\odot$.

The fraction of initial binaries is set to 0.2 :

$$f_b = \frac{N_b}{N_s + N_b} = 0.2 \tag{32}$$

where $N_b$ is the number of initial binaries (the number of stars initially in a binary being $2N_b$) and $N_s$ is the number of initially single stars. In other words, every third stars is initially in a binary because $2N_b/(2N_b + N_s) = 1/3$. Given that $N_s + 2N_b = 700$, there are 117 initial binaries and 466 initially single stars in the clusters. The distribution of initial semi-major axes of binaries $a$ is taken to be flat in $\log a$ between 1 and 1000 AU. In real clusters, binaries tighter than 1 AU and wider than 1000 AU exist. However, the tight ones can be considered as single objects. Hence they will not affect the dynamical evolution of the cluster. The wide ones are not considered because they break up very quickly and therefore their impact on planetary systems is not significant. The eccentricities of the initial binaries are distributed using a thermal distribution (Duquennoy and Mayor, 1991). For this distribution, the fraction $\mathrm{d}P(e)$ of binaries whose eccentricity is between $e$ and $\mathrm{d}e$ is given by

$$\mathrm{d}P(e) = 2e\,\mathrm{d}e. \tag{33}$$

Different samples of initial binaries properties of the same distributions are used for the 25 realizations carried out. As seen before, a star can also experience an exchange encounter in a binary during the run. If this binary breaks up very quickly, its impact on the planetary system is more similar to that caused by several fly-bys than to the effect of a binary companion. Therefore a bound system is defined as a binary only if it survives for at least five orbital periods. Otherwise, it is defined as a fly-by.

The stars are taken to be solar metallicity (Z = 0.02) and to evolve according to the stellar evolution prescription of Hurley et al. (2000).

Since the cluster is orbiting the galaxy, it is affected by its tidal force. The distance from the centre of the cluster where the central attraction of the cluster is balanced by the tidal force of the galaxy is called the tidal radius. For a star at a distance greater than the tidal radius from the centre of the cluster, the tidal force is higher than the cluster gravitational force. Thus this star will be ejected from the cluster. Therefore the tidal radius defines the spatial extension of the cluster. A standard tidal field (Aarseth, 2003) is used which consists to place the cluster on a circular orbit in the solar neighbourhood in the galaxy. The tidal radius is then given by

$$R_\mathrm{t} = \left[\frac{Gm_\mathrm{cl}}{4A(A-B)}\right]^{1/3} \tag{34}$$

where $m_\mathrm{cl}$ is the mass of the cluster. A and B, called Oort's constants, are related to the circular speed in the galaxy at a given distance from its centre. For the solar radius, the best estimates are A = 14.4 and B = -12.0 $\mathrm{kms^{-1}\,kpc^{-1}}$ (Binney and Tremaine, 1987). Hence the tidal radius is equal to 10.7 pc for $m_\mathrm{cl} = 425$ $\mathrm{M_\odot}$, which is the initial mass of the stars for the modelled cluster. Given that the initial half-mass radius of the cluster is 0.38 pc, the cluster is far from being tidally disrupted at that time.

## 4.2 Embedded clusters (with gas)

The properties of stars in modelled embedded clusters are the same as in dry ones. The same regularization criteria and the same criteria for fly-bys and binaries are used. The stars are taken to be initially in virial equilibrium i.e. the initial virial ratio of the stars is set to 0.5. $\alpha$ is defined by the initial ratio of the mass of the gas to the mass of the stars :

$$\alpha = \frac{m_{\rm gas}(0)}{m_\star}. \tag{35}$$

Simulations were performed for three values of $\alpha$ : 1, 3 and 9. Moreover, two gas removal timescales were used for $\alpha = 9$. 20 realizations were carried out for $\alpha = 1$ and 3 and 10 realizations for $\alpha = 9$. The number of realizations is lower for $\alpha = 9$ for technical reasons.

The gas follows the same Plummer density distribution as the stars of the cluster. More precisely, the initial density distribution of the stars and that of the gas are given by

$$\rho_\star(r) = \frac{3m_\star}{4\pi {r_0}^3}\left(1+\frac{r^2}{r_0^2}\right)^{-5/2} \tag{36}$$

and

$$\rho_{\rm gas}(r) = \frac{3m_{\rm gas}(0)}{4\pi {r_0}^3}\left(1+\frac{r^2}{r_0^2}\right)^{-5/2} \tag{37}$$

where the scaling factor $r_0$ is the same for both. The gas removal is modelled by an hyperbolic decrease of the mass of the gas. The evolution of the mass of the gas $m_{\rm gas}$ is given by

$$m_{\rm gas}(t) = \frac{m_{\rm gas}(0)}{1+\frac{t-t_{\rm exp}}{\tau_{\rm exp}}} \tag{38}$$

where $t_{\rm exp}$ is the time at which the gas removal begins and $\tau_{\rm exp}$ is the gas removal timescale. For all the runs, the gas removal begins at $t_{\rm exp} = 5$ Myr. For $\alpha = 1$ and 3, the gas removal timescale $\tau_{\rm exp}$ is taken to be 5 Myr. For $\alpha = 9$, two values of the gas removal timescale are used : 5 Myr and 1 Myr.

For technical reasons, the field force of the galaxy is not modelled in the same way as for dry clusters. The effects of the galactic disk and halo are modelled separately. The galactic disk is modelled by the potential of Miyamoto and Nagai (1975) given by

$$\Phi_{\rm disk}(R,z) = \frac{-GM_{\rm disk}}{\left\{R^2+\left[a+(b^2+z^2)^{1/2}\right]^2\right\}^{1/2}} \tag{39}$$

where $M_{\rm disk}$ is the mass of the galactic disk, $a$ and $b$ are linked to the dimensions of the disk and $R$ and $z$ are the radial and axial positions in the galaxy. The galactic halo is modelled by a logarithmic potential given by

$$\Phi_{\rm halo}(R) = V_0^2 \ln\left(\frac{R}{a_0}\right) \tag{40}$$

where $V_0$ and $a_0$ are two scaling factors depending on the halo mass and $R$ is the radial position in the galaxy. The field force is then obtained by computing the gradient of these potentials. As for dry clusters, the cluster is considered to be on a circular orbit in the solar neighbourhood in the galaxy.

# 5 Results

The results of the N-body simulations are presented in this section for dry clusters with five different values of the initial virial ratio Q and embedded clusters with three different values of the initial ratio of the mass of the gas to the mass of the stars $\alpha$. The evolution of the clusters is studied first. The main features of this evolution are pointed out for the different clusters. The impact of this evolution on the properties of encounters which occur during the run are determined. Afterwards, the encounters history of each star – fly-bys undergone and exchange encounters experienced – is studied. Furthermore, the number of singletons, i.e. initially single stars which never experience any encounters, is computed.

## 5.1 Dry clusters (without gas)

### 5.1.1 Clusters evolution

In this section, the evolution of the clusters is studied for the five values of the initial virial ratio Q. The main parameters which have to be considered are the half-mass radius, the virial ratio, the mass and the number of stars in the cluster. In order to examine their evolution, I modified the NBODY6 code to produce an output file containing the values of these parameters at different times. Afterwards, I produced a FORTRAN program to calculate the averages from the 25 realizations.

In the first place, the whole evolution of the cluster is studied. In figure 4, I plot the evolution of the half-mass radius of the cluster with time during the whole run for the five different values of Q. This evolution is similar for all the clusters. They expand rapidly during the first 200 Myr due to mass loss from stellar evolution. Then they stabilise at a half-mass radius of about 3 pc as obtained by Malmberg et al. (2007b) for the cluster initially in virial equilibrium (Q = 0.5). To study the early evolution of the clusters, I plot in figures 5 and 6 the evolution of the half-mass radius and virial ratio of the clusters with time during the first 10 Myr for the five values of Q. It appears that the main differences between the cluster initially in virial equilibrium (Q = 0.5) and those with subvirial initial conditions (Q < 0.5) are seen during this period. In figure 5, one can see that the initially subvirial clusters shrink in the first $\sim$ 1 Myr which is not the case for the initially virial one. Furthermore, this shrinking is more important for lower initial virial ratios. In these clusters, the initial velocity dispersion is too low for the stars to resist the central attraction of the cluster. Hence they fall towards the centre of the cluster with high velocities. The shrinking lasts $\sim$ 1 Myr which corresponds to the dynamical timescale of these clusters. These high velocities of the stars induce an increase of the virial ratio of the cluster as shown in figure 6. In the subsequent evolution, every cluster expands. For initially subvirial clusters, this expansion is enhanced by the shrinking. Therefore it is faster for lower Q. During this period, the virial ratio reaches a roughly constant value close to 0.5 for all the clusters.

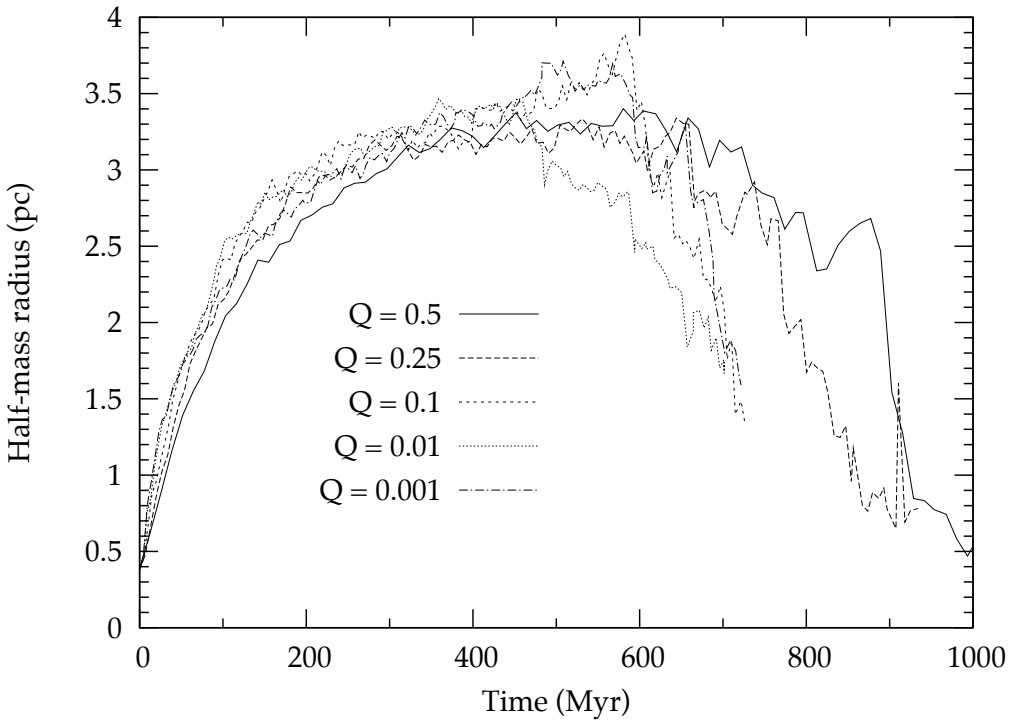


Figure 4: Evolution of the half-mass radius of the cluster with time during the whole run for different values of the initial virial ratio : Q = 0.5, 0.25, 0.1, 0.01 and 0.001. The value of the half-mass radius is the average from the 25 realizations ran for each cluster.

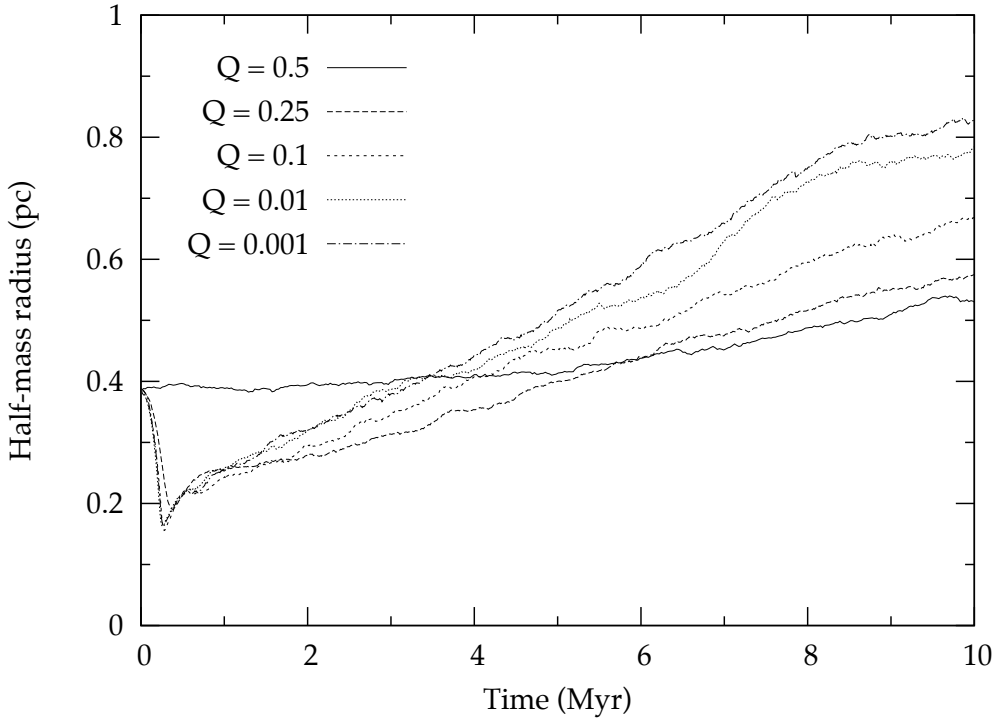


Figure 5: Evolution of the half-mass radius of the cluster with time during the first 10 Myr for different values of the initial virial ratio : Q = 0.5, 0.25, 0.1, 0.01 and 0.001. The value of the half-mass radius is the average from the 25 realizations ran for each cluster.

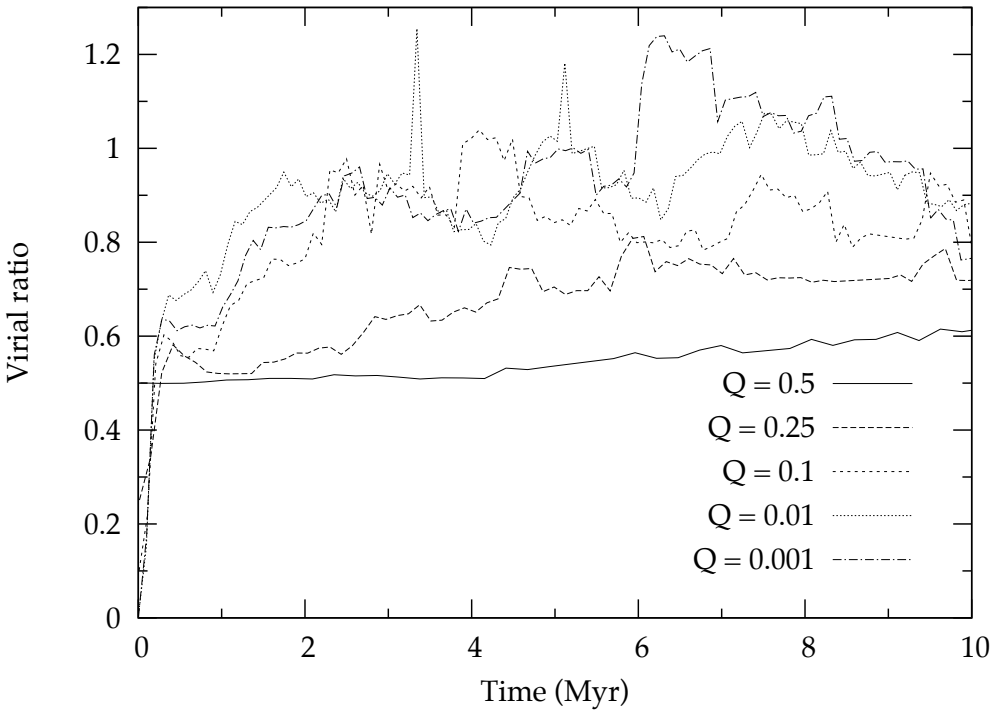


Figure 6: Evolution of the virial ratio of stars in the cluster with time for different values of the initial virial ratio : Q = 0.5, 0.25, 0.1, 0.01 and 0.001. The value of the virial ratio is the average of the 25 realizations ran for each cluster.

To evaluate the mass loss from the clusters, I plot in figure 7 the evolution of the mass and number of stars with time for the five values of Q. The clusters undergo a significant mass loss in the first 50 Myr which is more important for lower Q. For these clusters, the increase of the velocities of the stars due to the initial shrinking causes some of them to escape. The decrease in the number and mass of stars, is roughly constant with time after 50 Myr for all the initial virial ratios. This evolution is consistent with that found by Malmberg et al. (2007b) for Q = 0.5. One can also see that the number of stars decreases more rapidly than the mass of the stars. It means that low-mass stars are lost more rapidly than massive ones. When energy equipartition is achieved due to two-body relaxation, the velocities of the less massive stars are higher and can exceed the escape velocity of the cluster. An additional effect of energy equipartition is called mass segregation. It will be studied in section 6.3.

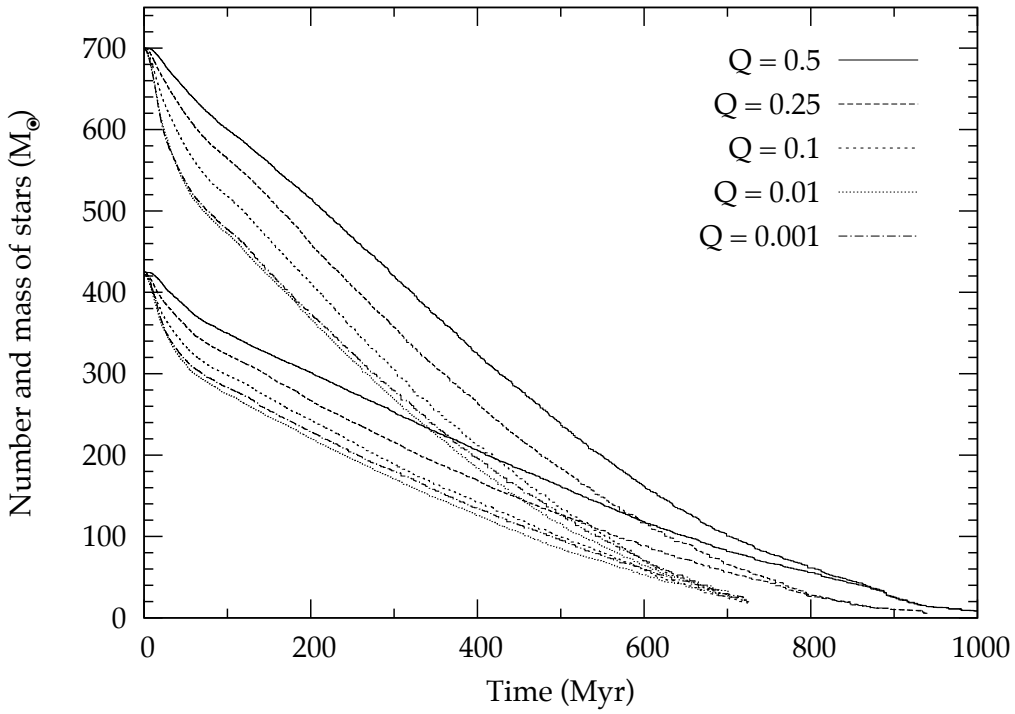


Figure 7: Evolution of the mass and number of stars in the cluster with time for different values of the initial virial ratio : Q = 0.5, 0.25, 0.1, 0.01 and 0.001. The values of the mass and number of stars are the average from the 25 realizations ran for each cluster.

### 5.1.2 Rate and closest approaches of fly-bys

As seen previously, the initially subvirial clusters (Q < 0.5) shrink in the first $\sim$ 1 Myr and this shrinking is followed by a phase of expansion. However, the virial cluster (Q = 0.5) does not shrink and expands very slowly. Given this evolution of the clusters, it is interesting to study how it influences the rate of fly-bys involving initially single stars. It will be seen in the following that this rate has an influence on the evolution of the number of singletons. Furthermore, to study how are affected the planetary systems whose host-star experience a fly-by, it is worth knowing the distribution of the periastrons of fly-bys involving initially single stars. Because only one close fly-by can highly affect a planetary system, it is also important to evaluate the number of initially single stars which undergo at least one fly-by at a given distance.

To study the encounter rate, I wrote a FORTRAN program which prints the properties of every fly-by which occurs during a run. Then I produced a program to compute the evolution of the cumulative fraction of fly-bys involving initially single stars. I also calculated the number of fly-bys which happen in the first 10 Myr. It allowed me to know the evolution of the cumulative number of fly-bys experienced by initially single stars in the first 10 Myr. Finally, I calculated the average value from the 25 realizations realized for each cluster.

I plot in figure 8 the evolution of the cumulative number of fly-bys experienced by initially single stars in the first 10 Myr with time for the five values of Q. According to equation 22, the encounter timescale is proportional to ${r_{\rm h}}^{5/2}$. Hence the encounter rate is higher during the shrinking of the cluster which lasts $\sim$ 1 Myr. As this shrinking

is more important for lower virial ratios, the encounter rate is higher for lower initial virial ratios during this period. The subsequent expansion leads to a decrease of the encounter rate for initially subvirial clusters. As the initially virial cluster does not shrink and expands very slowly during the first 10 Myr, its encounter rate is constant in this period. During the later evolution (from 10 Myr to the disruption of the clusters), all the clusters highly expand and undergo a mass loss (figures 4 and 7). As the encounter timescale is proportional to ${r_{\rm h}}^{5/2}$ and also to ${m_{\rm cl}}^{-1/2}$ according to equation 22, it leads to an important decrease of the encounter rate. Hence, especially for initially subvirial clusters, the majority of the encounters occurs during the first 10 Myr. As it will be shown in the following, it causes the majority of the non-singletons to be produced in this period.

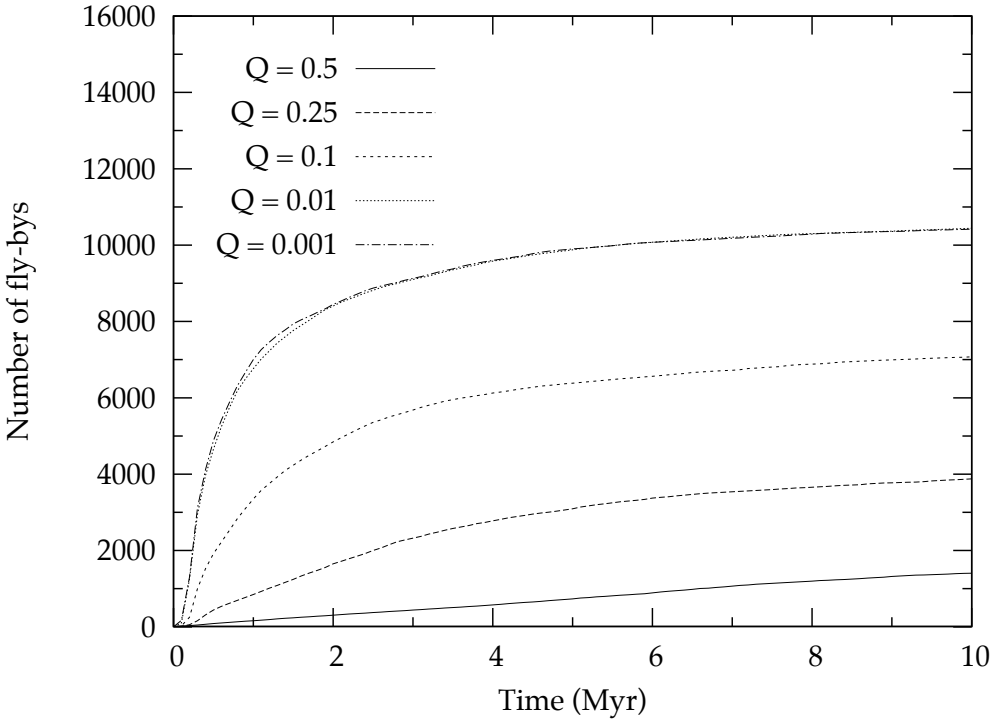


Figure 8: Evolution of the cumulative number of fly-bys experienced by initially single stars in the first 10 Myr with time for different values of the virial ratio Q : 0.5, 0.25, 0.1, 0.01 and 0.001. The number of fly-bys is the average value from the 25 realizations ran for each cluster.

To know the periastron distribution of fly-bys involving initially single stars, I produced a FORTRAN program to calculate the cumulative fraction of fly-bys as a function of the periastron during the first 10 Myr. Then I calculated the number of fly-bys which occur during this period and I deduced the cumulative number of fly-bys as a function of their periastron in the first 10 Myr. To know how many stars experience at least one fly-by at a given distance, I also wrote a FORTRAN program to calculate the minimum closest distance of fly-bys experienced by each star.

I plot in figure 9 the number of fly-bys experienced by initially single stars during the first 10 Myr as a function of their periastron. For all the clusters, one can see that it is proportional to $r_{\rm min}$ according to equation 19 because of the gravitational focussing.

Besides the number of these fly-bys is higher for lower Q due to the higher encounter rate.

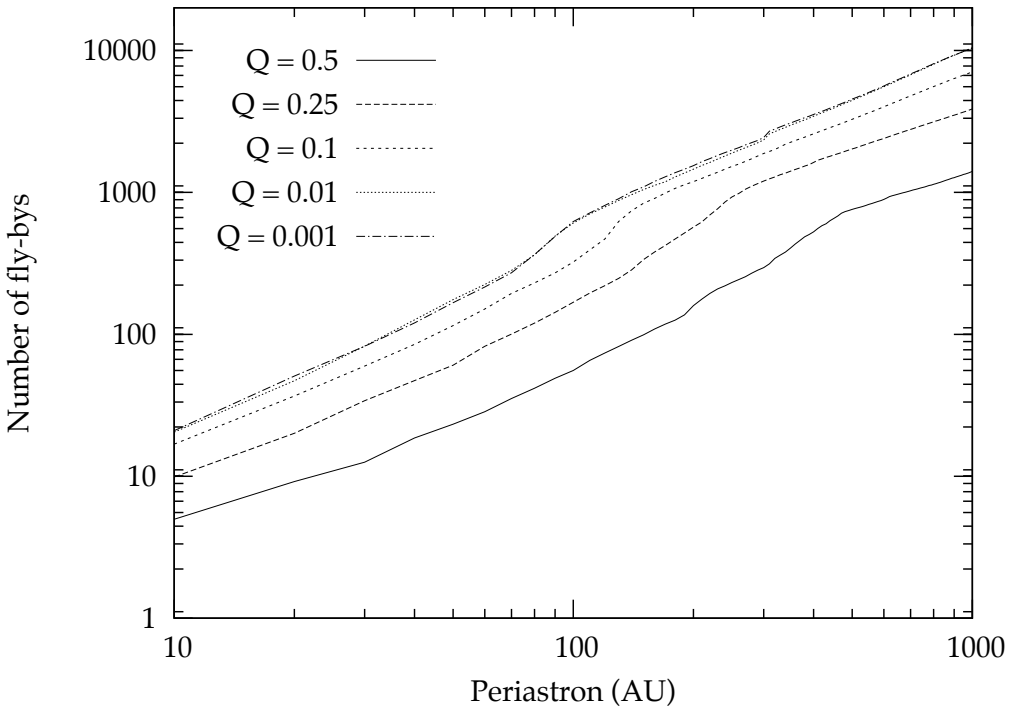


Figure 9: Cumulative number of fly-bys experienced by initially single stars in the first 10 Myr as a function of their periastron for different values of the virial ratio Q : 0.5, 0.25, 0.1, 0.01 and 0.001. The number of fly-bys is the average value from the 25 realizations ran for each cluster.

I plot in figures 10 and 11 the number and fraction of initially single stars which experience fly-bys in the first 10 Myr with the minimum closest distance of these fly-bys for the five values of Q. Even if a star experiences a lot of fly-bys, only the tight ones (with $r_{\rm min} < 100\,{\rm AU}$) are likely to perturb its planetary system. Hence one has to focus on these fly-bys. The fraction of initially single stars that experience at least one fly-by with $r_{\rm min} < 100\,{\rm AU}$ is 0.08 for Q = 0.5, 0.14 for Q = 0.25, 0.21 for Q = 0.1, 0.25 for Q = 0.01, 0.26 for Q = 0.001. These results will be used in sections 6.1 and 6.2 where effects of fly-bys on different sorts of planetary systems and planets are described.

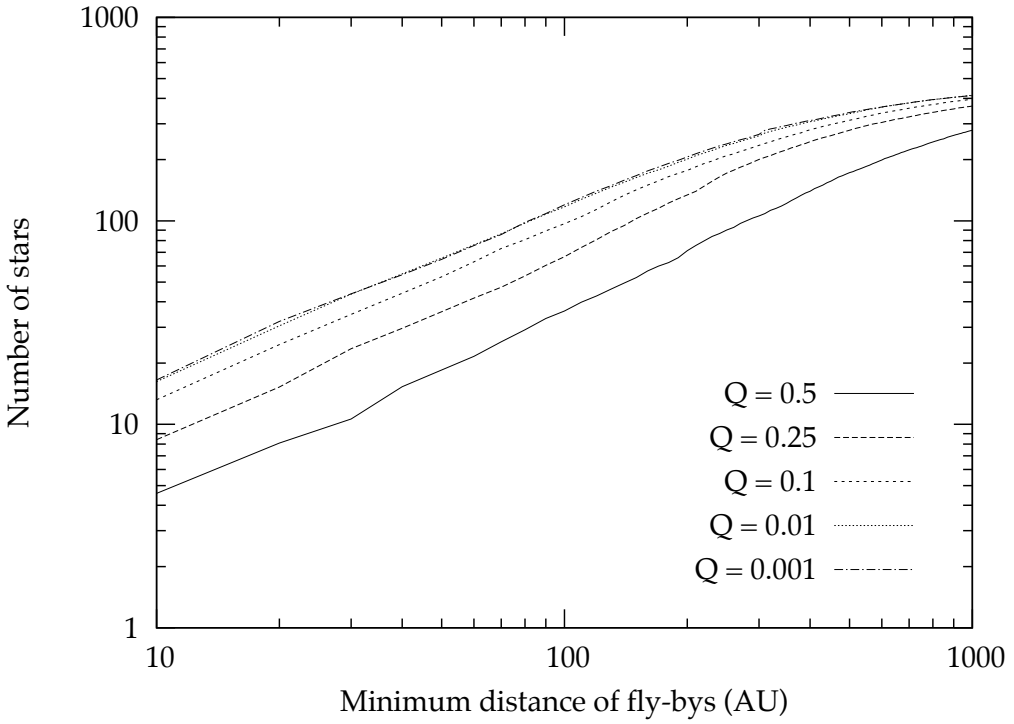


Figure 10: Cumulative number of initially single stars which experience fly-bys in the first 10 Myr with the minimum closest distance of these fly-bys for different values of the virial ratio Q : 0.5, 0.25, 0.1, 0.01 and 0.001. The number of stars is the average value from the 25 realizations ran for each cluster.

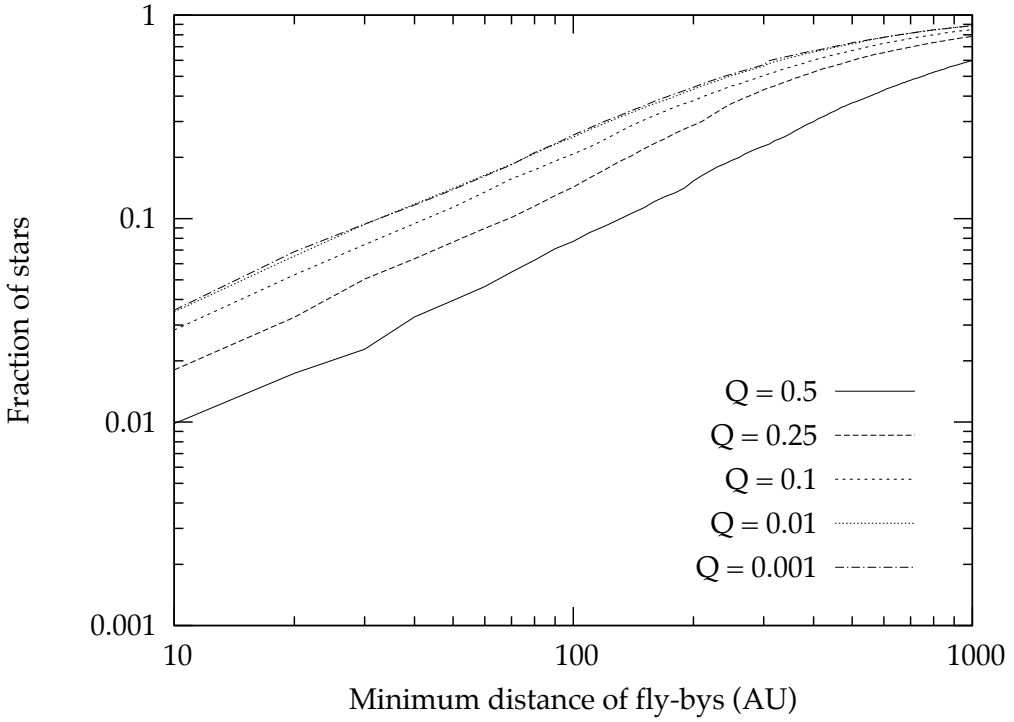


Figure 11: Fraction of initially single stars which experience fly-bys in the first 10 Myr with the minimum closest distance of these fly-bys for different values of the virial ratio Q : 0.5, 0.25, 0.1, 0.01 and 0.001. The fraction is the average value from the 25 realizations ran for each cluster.

### 5.1.3 Binaries properties

Another mechanism that impacts on planetary systems is the exchange encounter of their host star. As for fly-bys, the clusters evolution affects the exchange encounter rate. To study it, I wrote a FORTRAN program to extract the properties of exchange encounters which occur during each run. The analysis programs that I wrote to determine the rate and the distribution of exchange encounter with their periastron in the first 10 Myr are similar to those used for fly-bys.

I plot in figure 12 the evolution of the number of exchange encounters experienced by initially single stars in the first 10 Myr for the five values of Q. As seen before, the encounter rate in the initially subvirial clusters is higher when they shrink in the first $\sim$ 1 Myr. As an exchange encounter occurs after a three-body interaction, the number of exchange encounter depends on this encounter rate. Hence the exchange encounter rate is higher for lower Q in this period.

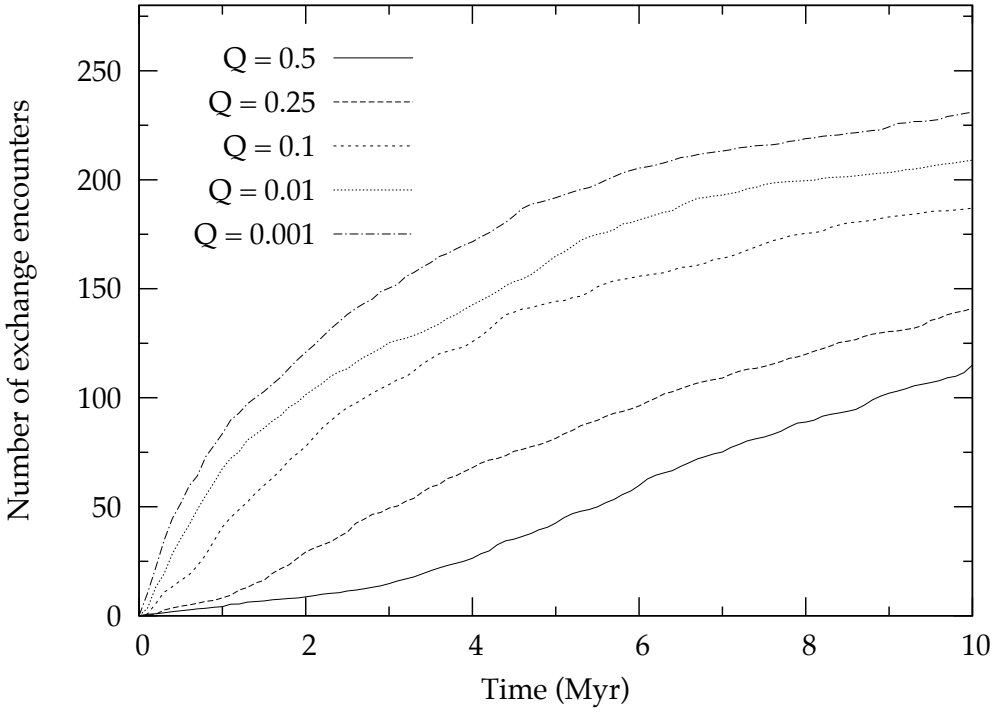


Figure 12: Evolution of the number of exchange encounters experienced by initially single stars in the first 10 Myr with time for different values of the virial ratio Q : 0.5, 0.25, 0.1, 0.01 and 0.001. The number is the average value from the 25 realizations ran for each cluster.

The number and fraction of initially single stars which experience at least one exchange encounter during the first 10 Myr are shown in table 1. One can notice that only a low fraction (less than 13 %) of initially single stars are involved in an exchange encounter. However, Malmberg et al. (2007a) found that the binary component is likely to have a high inclination with respect to the orbit planes of the planetary system. More precisely, for 77 % of the binaries formed by an exchange encounter, this inclination is sufficient for the Kozai mechanism to occur. Therefore, even if the fraction of stars involved in an exchange encounter is low, the fraction of planetary systems affected by

this mechanism is likely to be significant. This post-encounter effect will be studied in further detail in section 6.1.

| Virial ratio | Number of stars which exchange in a binary | Fraction of stars which exchange in a binary |
|---|---|---|
| 0.5 | 33 | 0.07 |
| 0.25 | 43 | 0.09 |
| 0.1 | 43 | 0.09 |
| 0.01 | 55 | 0.12 |
| 0.001 | 62 | 0.13 |

Table 1: Number and fraction of initially single stars which experience at least one exchange encounter during the first 10 Myr for different values of the virial ratio Q : 0.5, 0.25, 0.1, 0.01 and 0.001. The number and fraction of stars are the average values from the 25 realizations ran for each cluster.

### 5.1.4 Impact on planetary systems

To quantify the effect of fly-bys and exchange encounters on planetary systems, it is interesting to know the encounter history of each star in the clusters in the first 10 Myr. Indeed, the majority of the encounters occur in this period as seen previously. A practical way to evaluate the history of each star is to build a Venn diagram. An example of such diagrams can be seen in figure 13. The upper circle contains the percentage of stars which are single at the end of the first 10 Myr (S), the lower left circle the percentage of stars which experience an exchange encounter in a binary in the first 10 Myr (B) and the lower right circle the percentage of the stars which have a close encounter during the first 10 Myr (F). To obtain these diagrams, I began by modifying the NBODY6 code to produce an output file containing the encounter history of every star in the clusters. Afterwards, I wrote a FORTRAN program to determine for every initially single star in which category it has to be placed. Finally, I calculated the averages from the 25 realizations. Categories of the Venn diagram are defined by the criteria given in section 4. An example is the criterion for binaries: a bound system has to survive for at least five orbital periods to be counted as a binary. To take it into account, I computed the lifetimes of all the bound systems. Afterwards, I calculated the orbital periods of these systems by the Kepler third law, the masses of the components being in an output file of the NBODY6 code. Furthermore, it is also interesting to study how the number of singletons depends on the clusters evolution. Hence one needs to know the evolution of this number with time. That is why I wrote another program which compute this number for different times.

Venn diagrams are shown in figure 13. They give the encounter histories in the first 10 Myr of all the stars which are initially single in the cluster for different values of the initial virial ratio Q : 0.5, 0.25, 0.1, 0.01, 0.001. The results are also summarized in table 2. The percentages can be converted in numbers given that there are 466 initially single stars in the clusters. On can see, according to the previous discussions, that the percentage of initially single stars which experience a fly-by (FS) increases when the initial virial ratio decreases : 52.8 % for Q = 0.5 and 77.7 % for Q = 0.001. Similarly,

the percentage of initially single stars which experience a exchange encounter (FSB and FB) increases when the initial virial ratio decreases : 4.8 % and 2.3 % for Q = 0.5 and 8.5 % and 4.9 % for Q = 0.001. Hence the percentage of singletons at the end of the first 10 Myr is lower for lower initial virial ratios : 40.1 % for Q = 0.5 and 8.9 % for Q = 0.001. One can see that one given initially single star experience much more fly-bys than exchange encounters. However, the post-encounter effect on planetary systems is not the same for these two categories of encounters. As seen before, only a low fraction of fly-bys (those with a minimum distance $r_{\min} < 100\,\mathrm{AU}$) causes a significant perturbation of the planetary systems. However, Kozai mechanism occurs for a large fraction of exchange encounters (77 %). This effect will be studied in further detail in section 6.1.

The evolution of the number of singletons is given by figure 14 as a function of time in the first 10 Myr. Because of the higher encounter rate for clusters with Q < 0.5, the number of singletons drops steeply during this period. However, this decrease is more smooth for the initially virial cluster because the encounter rate is lower. Furthermore, the number of singletons appears to be stable at the end of the first 10 Myr especially for subvirial clusters. It means that the majority of non-singletons are created in this period.

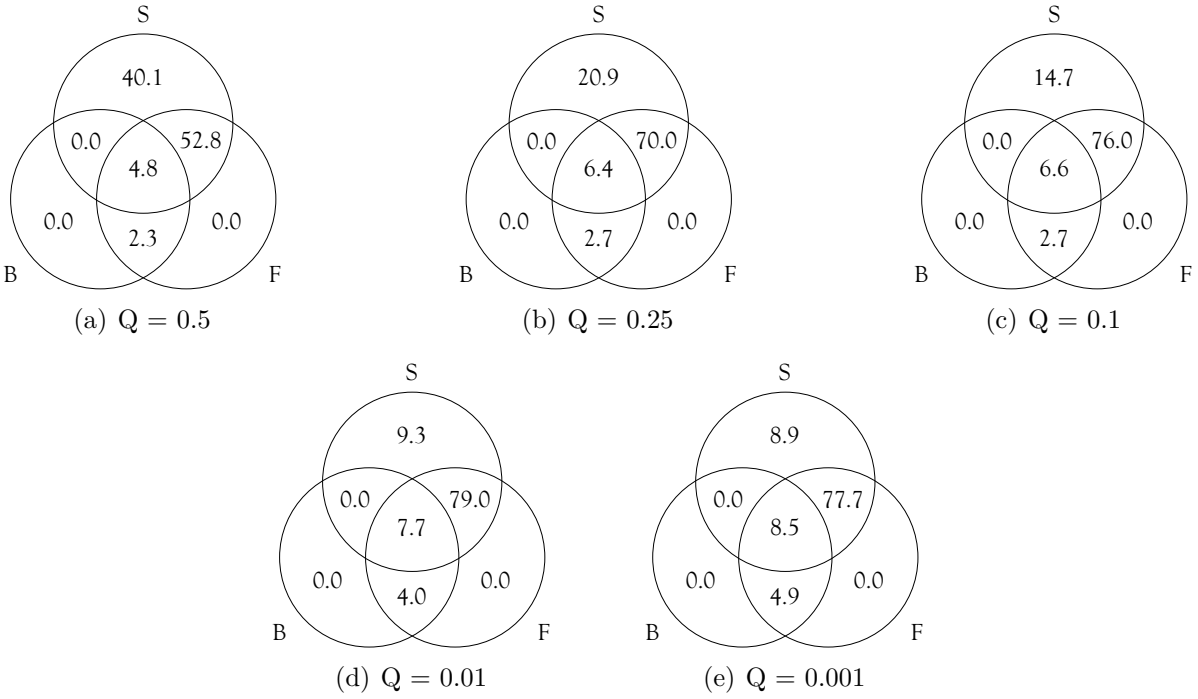


(a) Q = 0.5 (b) Q = 0.25 (c) Q = 0.1

(d) Q = 0.01 (e) Q = 0.001

Figure 13: Venn diagrams of the stars which are initially single in the cluster for Q = 0.5, 0.25, 0.1, 0.01 and 0.001 at the end of the first 10 Myr. The upper circle contains the percentage of stars which are single at the end of the first 10 Myr (S), the lower left circle the percentage of stars which experience an exchange encounter in a binary during the first 10 Myr (B) and the lower right circle the percentage of the stars which have a close encounter during the first 10 Myr (F). The percentages are the averaged values for the 25 realizations.

| Q | 0.5 | 0.25 | 0.1 | 0.01 | 0.001 |
|---|---|---|---|---|---|
| S | 40.1 ± 2.4 | 20.9 ± 2.4 | 14.7 ± 1.6 | 9.3 ± 2.7 | 8.9 ± 1.9 |
| FS | 52.8 ± 2.3 | 70.0 ± 2.0 | 76.0 ± 1.6 | 79.0 ± 2.9 | 77.7 ± 2.9 |
| FSB | 4.8 ± 1.1 | 6.4 ± 1.4 | 6.6 ± 1.3 | 7.7 ± 1.6 | 8.5 ± 2.0 |
| FB | 2.3 ± 0.7 | 2.7 ± 0.7 | 2.7 ± 0.9 | 4.0 ± 1.2 | 4.9 ± 1.4 |
| F | 0.0 ± 0.0 | 0.0 ± 0.0 | 0.0 ± 0.0 | 0.0 ± 0.0 | 0.0 ± 0.0 |
| B | 0.0 ± 0.0 | 0.0 ± 0.0 | 0.0 ± 0.0 | 0.0 ± 0.0 | 0.0 ± 0.0 |
| SB | 0.0 ± 0.0 | 0.0 ± 0.0 | 0.0 ± 0.0 | 0.0 ± 0.0 | 0.0 ± 0.0 |

Table 2: Percentage of the stars for each category of the Venn diagram 10 Myr after the beginning of the run for different values of the virial ratio : Q = 0.5, 0.25, 0.1, 0.01 and 0.001. The percentages are the averaged values for the 25 realizations. The error bars are the standard deviations.

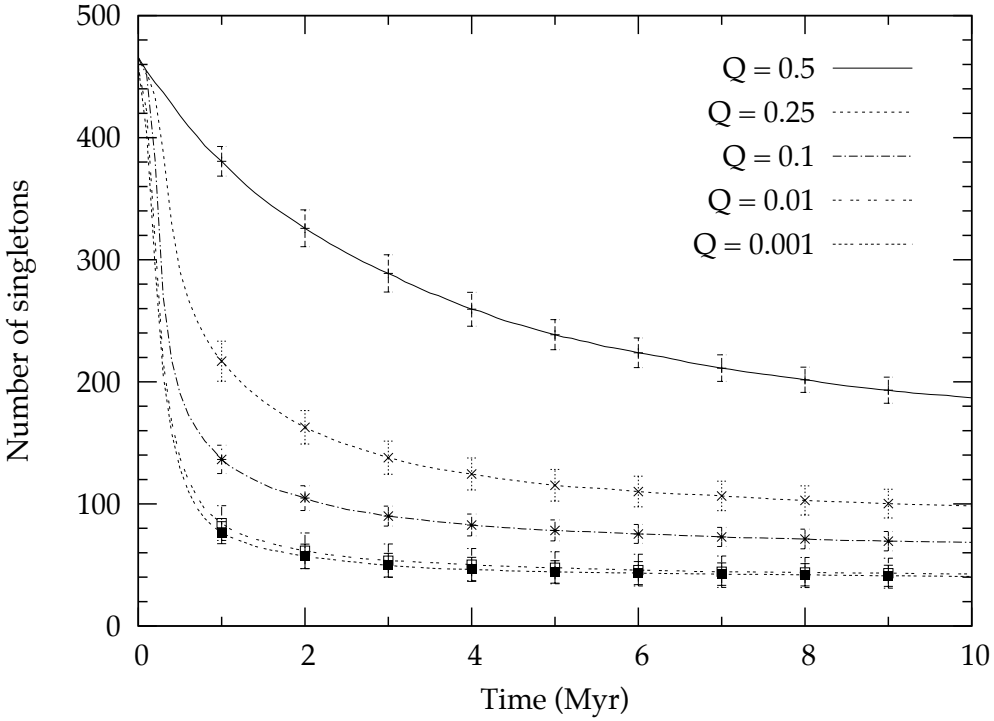


Figure 14: Evolution of the number of singletons with time for different values of the virial ratio Q : 0.5, 0.25, 0.1, 0.01 and 0.001. The number of singletons is the average value from the 25 realizations ran for each cluster. The error bars are the standard deviations.

### 5.1.5 Influence of initial positions

As discussed previously, the number of singletons at the end of the first 10 Myr is highly influenced by the clusters evolution. It is also interesting to evaluate the impact of initial conditions on this number. The two main initial conditions which are likely to influence the number of singletons are the initial radial positions in the cluster and the initial distances of the nearest neighbour for each star. Hence one needs to know the distributions of these distances for stars which are singletons and those which are non-

singletons at the end of the first 10 Myr. To do so, I produced a FORTRAN program to determine if a star is a singleton at the end of the first 10 Myr. The NBODY6 code automatically produce an output file with the initial coordinates of the stars. I wrote two programs to calculate the distribution of the initial radial and nearest neighbour distances from this output file for singletons and non-singletons. Finally, I computed the average value from the 25 realizations.

The results are presented in figures 15 and 16 for the initially virial cluster. As one can see in these figures, singletons tend to be initially further from the centre of the cluster and to have further neighbours than the non-singletons. These initial conditions prevent them from experiencing a fly-by or an exchange encounter in the first 10 Myr.

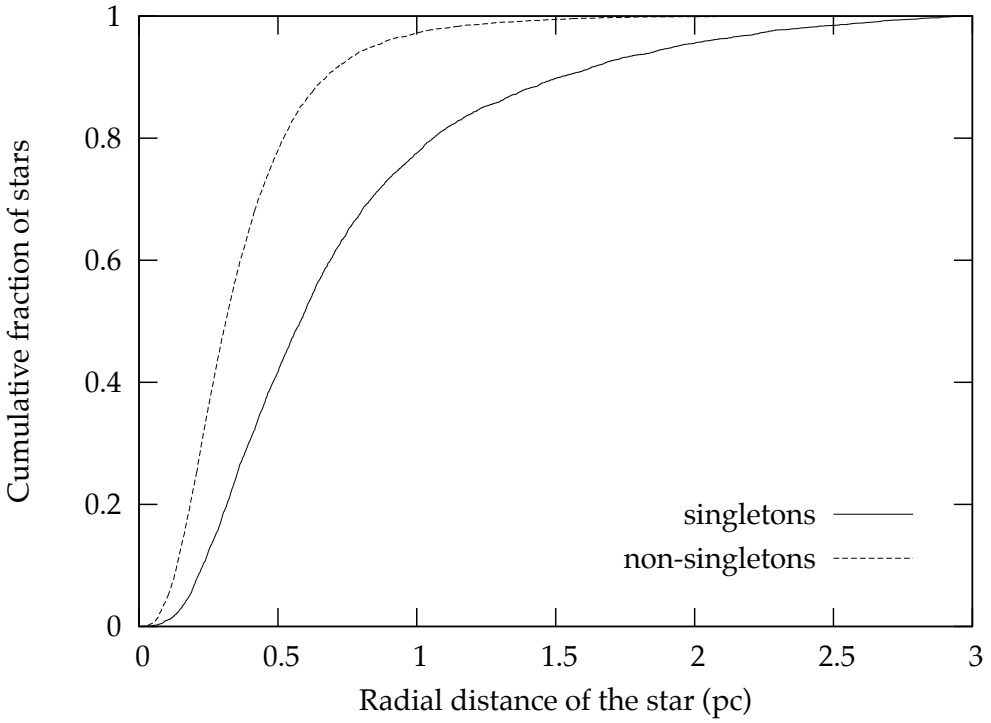


Figure 15: Cumulative fraction of stars as a function of their initial radial position in the initially virial cluster. The fraction is calculated for stars which are singletons and those which are non-singletons at the end of the first 10 Myr.

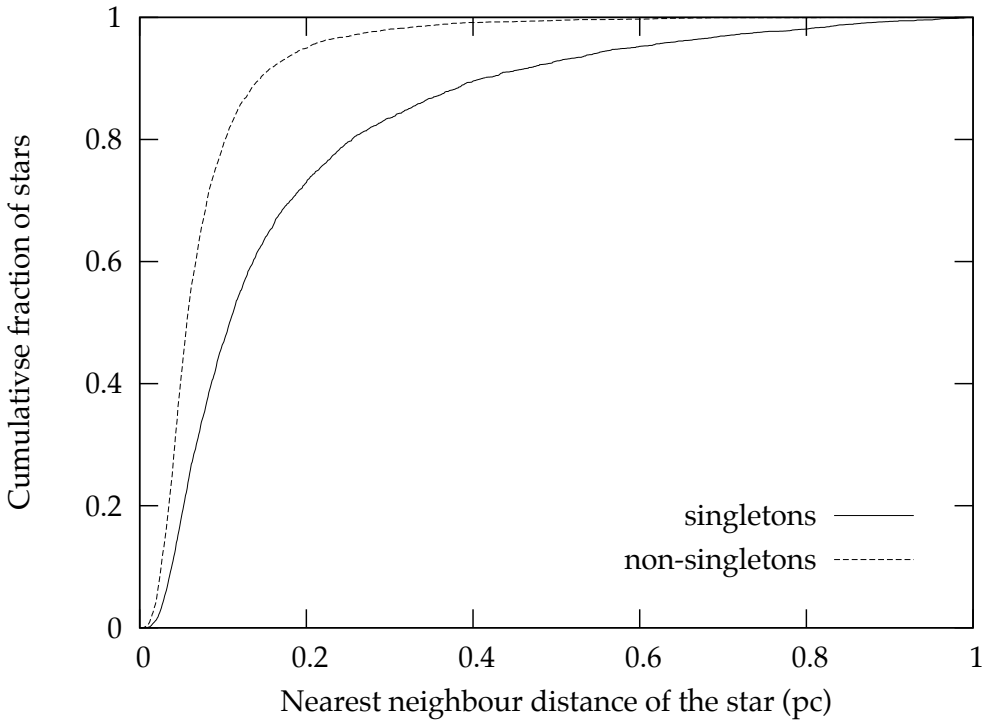


Figure 16: Cumulative fraction of stars in the initially virial cluster as a function of the initial distance of their nearest neighbour. The fraction is calculated for stars which are singletons and those which are non-singletons at the end of the first 10 Myr.

## 5.2 Embedded clusters (with gas)

### 5.2.1 Clusters evolution

In this section, the evolution of the clusters is studied for the three initial ratios of the mass of the gas to the mass of the stars $\alpha$ and the two removal timescales for $\alpha = 9$. The main parameters are the mass of the gas in the cluster, the half-mass radius and the virial ratio of the stars i.e. the ratio of the kinetic energy of the stars to their potential energy. The FORTRAN programs that I wrote to obtain the evolution of these parameters are very similar to those used for dry clusters. The average is computed from the 20 and 10 realizations carried out for $\alpha = 1$ and 3 and $\alpha = 9$ respectively.

I plot in figure 17 the evolution of the mass of the gas. It evolves according to equation 38 where the gas removal begins at $t_{\rm exp} = 5$ Myr. For $\alpha = 1$ and 3, the gas removal timescale $\tau_{\rm exp}$ is taken to be 5 Myr. For $\alpha = 9$, two values of the gas removal timescale were used : 5 Myr and 1 Myr. The latter will be called rapid in the following.

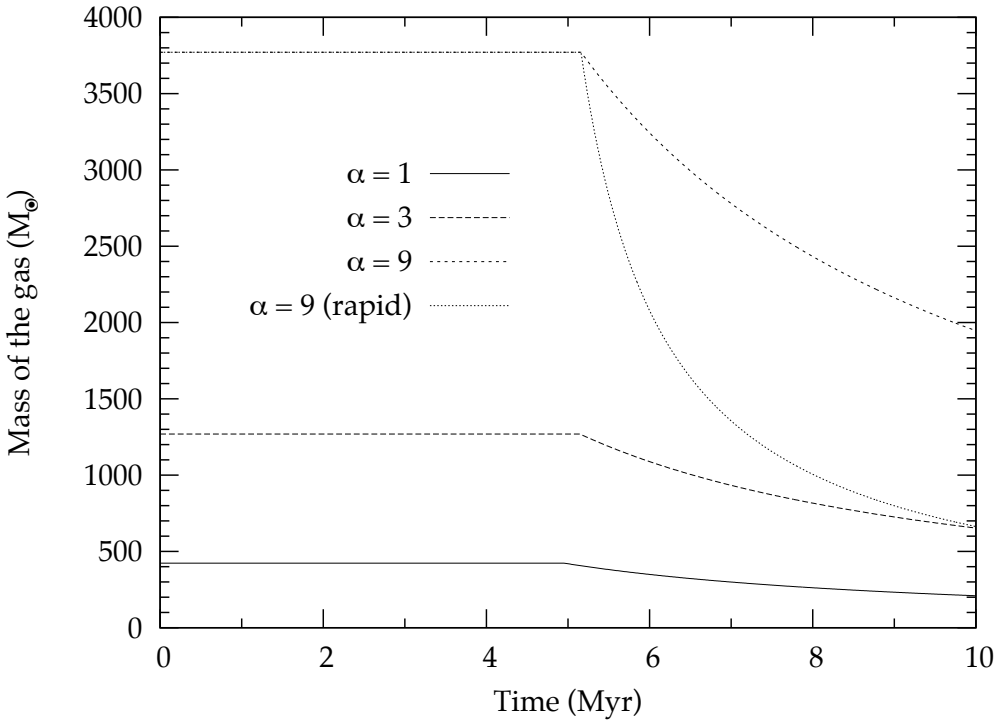


Figure 17: Evolution of the mass of the gas in the cluster with time for different values of the initial ratio of the mass of the gas to the mass of the stars $\alpha$ : 1, 3 and 9. The value of the mass of the gas is the average from the 20 realizations ran for $\alpha = 1$ and 3 and the 10 realizations ran for $\alpha = 9$.

I plot the half-mass radius and the virial ratio of the stars in figures 18 and 19. All the clusters shrink in the first $\sim$ 1 Myr. This shrinking is more substantial for higher $\alpha$. Because of the presence of the gas, the initial velocity dispersion is too low for the stars to resist the central attraction of the cluster. Hence, the velocities of the stars increase. It induces an rise of the virial ratio of the stars as can be seen in figure 19. Afterwards, the half-mass radius reaches a constant value for every cluster. The equilibrium half-mass radius is greater for lower $\alpha$ because the central attraction of the gas is lower. Similarly, the virial ratio of the stars reaches a constant value which is greater for higher $\alpha$. Indeed, the higher the mass of the gas is, the higher the velocities of the stars are when the virial equilibrium is achieved for the whole cluster. When the gas is expelled at 5 Myr, the cluster expands because the potential of the gas decreases. This expansion is faster for a rapid gas removal as can be seen in figure 18. In this period, the velocities of the star decrease because the gravitational potential is lower. Therefore their virial ratios decrease as can be seen in figure 19.

The number of stars ejected from the clusters is not significant in the first 10 Myr. Indeed, they did not expand enough at that time to be tidally disrupted. For technical reasons, the evolution of these clusters cannot be modelled sufficiently long to see their disruption.

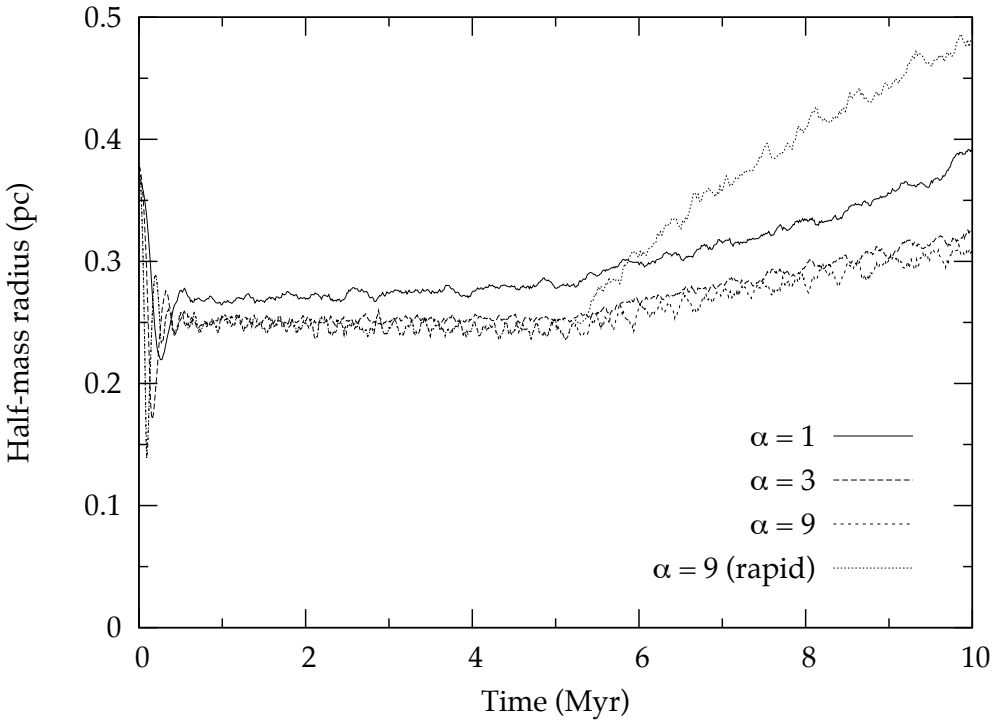


Figure 18: Evolution of the half-mass radius of the cluster with time for different values of the initial ratio of the mass of the gas to the mass of the stars $\alpha$ : 1, 3 and 9. The value of the half-mass radius is the average from the 20 realizations ran for $\alpha = 1$ and 3 and the 10 realizations ran for $\alpha = 9$.

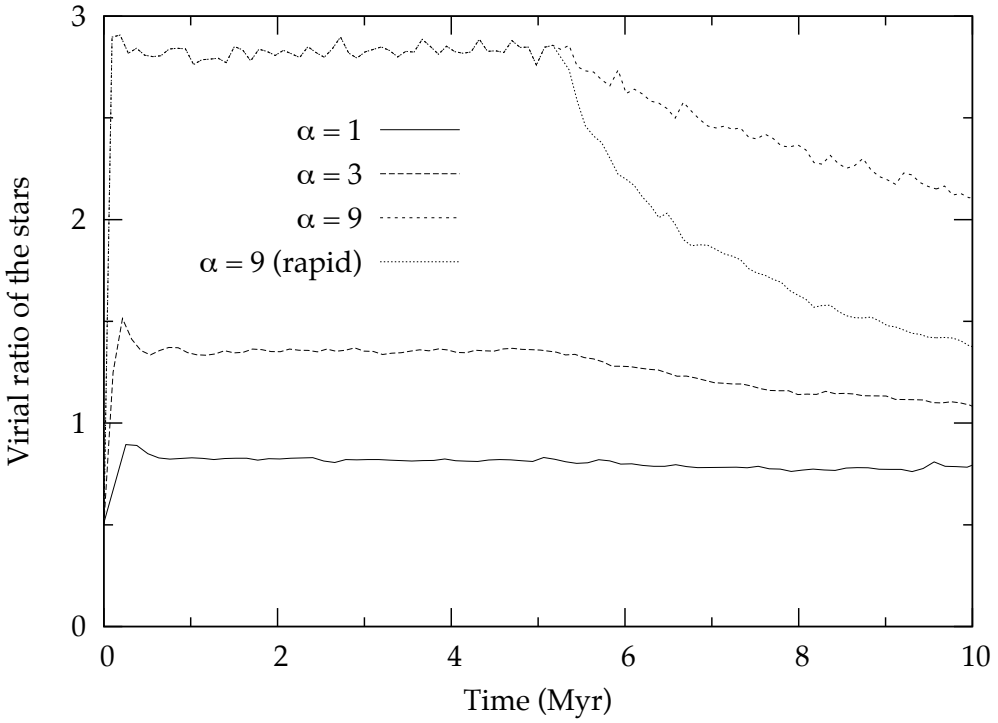


Figure 19: Evolution of the virial ratio of the stars with time for different values of the initial ratio of the mass of the gas to the mass of the stars $\alpha$ : 1, 3 and 9. The value of the virial ratio is the average from the 20 realizations ran for $\alpha = 1$ and 3 and the 10 realizations ran for $\alpha = 9$.

### 5.2.2 Rate and closest approaches of fly-bys

As seen before, the clusters shrink in the first $\sim 1$ Myr and keep a constant half-mass radius before the gas expulsion. The shrinking is more important for higher $\alpha$ and the equilibrium half-mass radius is lower. As for dry clusters, it is interesting to study how this evolution affect the rate of fly-bys involving initially single stars and to evaluate the periastron distribution of these fly-bys in the first 10 Myr. The FORTRAN programs realized are similar to those used for dry clusters in the corresponding section.

I plot in figure 20 the number of fly-bys experienced by initially single stars in the first 10 Myr with time for different values of $\alpha$. According to equation 22, the encounter timescale is proportional to ${r_{\rm h}}^{5/2}$. Hence the encounter rate is roughly constant and greater for higher $\alpha$ due to the constant half-mass radius before the gas expulsion. The gas removal at 5 Myr causes an expansion of the cluster. Therefore it involves a decrease of the encounter rate which is is more important for the fast gas removal.

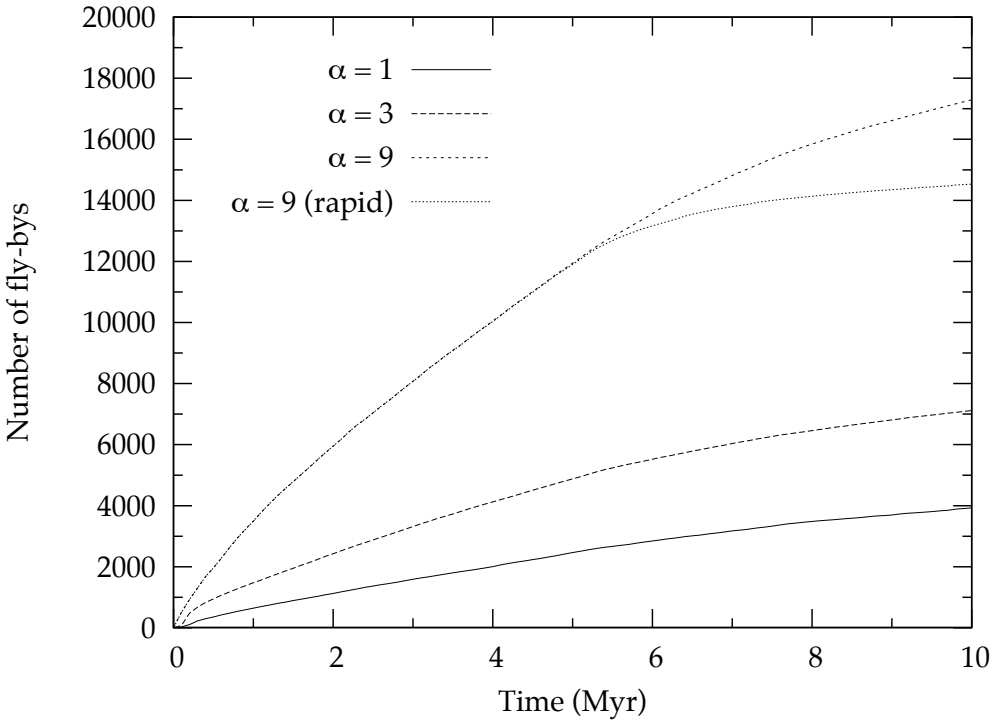


Figure 20: Evolution of the cumulative number of fly-bys experienced by initially single stars in the first 10 Myr with time for different values of the initial ratio of the mass of the gas to the mass of the stars $\alpha$ : 1, 3 and 9. The value of the virial ratio is the average from the 20 realizations ran for $\alpha = 1$ and 3 and the 10 realizations ran for $\alpha = 9$.

In figure 21, I plot the number of fly-bys experienced by initially single stars in the first 10 Myr as a function of their periastron for different values of $\alpha$. One can see that this number evolves more steeply for clusters with high $\alpha$ than for dry clusters. This effect can be accounted for as follows. The potential of the gas is higher for clusters with greater $\alpha$. Therefore the velocity dispersion in these clusters is higher. As a consequence, equation 19 can not be used to evaluate the probability of encounters as it was

the case for dry clusters. In clusters with high $\alpha$, there are fly-bys which are not dominated by gravitational focussing. During these fly-bys, the relative velocity of the two stars at closest approach is lower than the velocity dispersion. Hence, the cross-section for two stars to experience these fly-bys is given by equation 20. These fly-bys are likely to happen between low-mass stars and within a high minimum distance (equation 18).

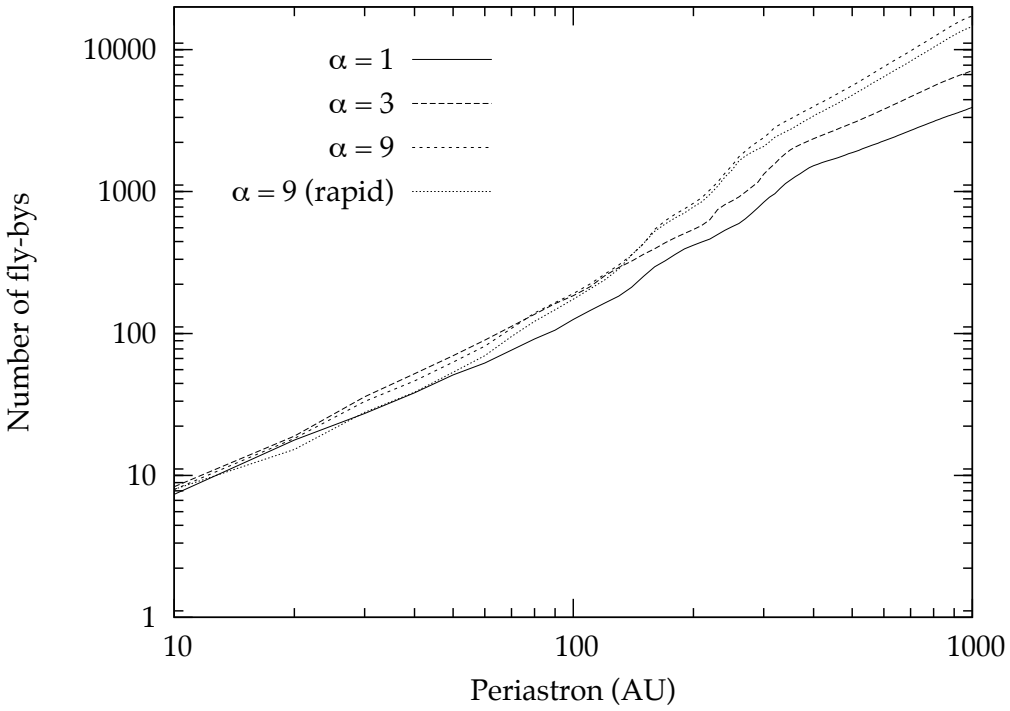


Figure 21: Cumulative number of fly-bys experienced by initially single stars in the first 10 Myr as a function of their periastron for different values of the initial ratio of the mass of the gas to the mass of the stars $\alpha$ : 1, 3 and 9. The value of the virial ratio is the average from the 20 realizations ran for $\alpha = 1$ and 3 and the 10 realizations ran for $\alpha = 9$.

I plot in figures 22 and 23 the number and fraction of initially single stars which experience fly-bys in the first 10 Myr with the minimum closest distance of these fly-bys for the five values of $\alpha$. Among all the fly-bys experienced by an initially single star, only the tight ones (with $r_{\rm min} < 100\,{\rm AU}$) are likely to lead to an ejection of planet from its planetary system. The fraction of initially single stars which experience at least one of these fly-bys is 0.14 for $\alpha = 1$, 0.18 for $\alpha = 3$, 0.27 for $\alpha = 9$ and 0.23 for $\alpha = 9$ with a rapid gas removal. This result will be used in sections 6.1 and 6.2 where the effects of fly-bys on different sorts of planetary systems and planets are described.

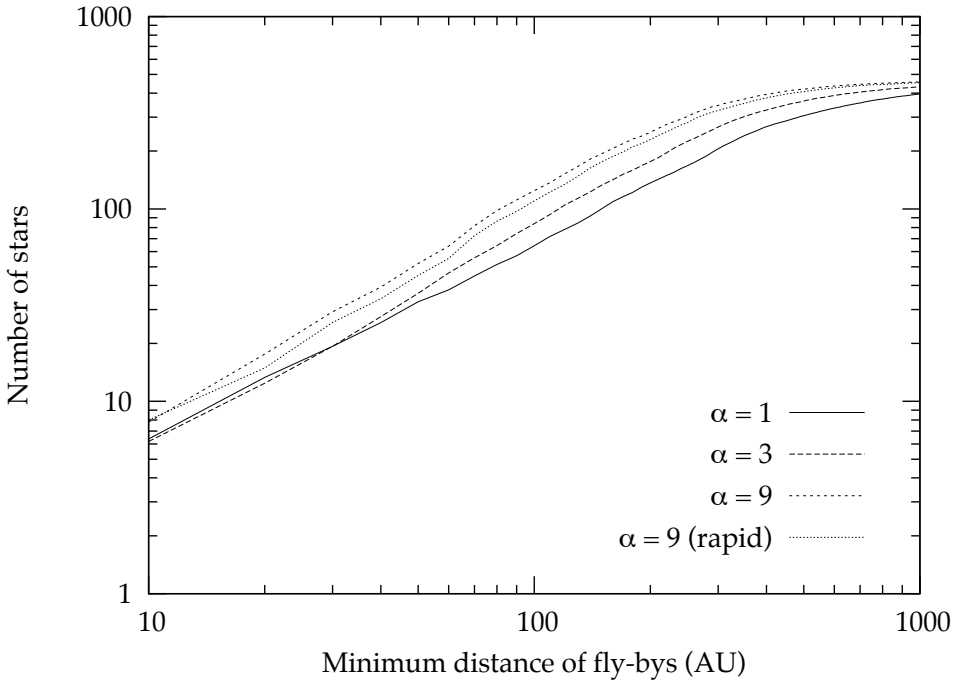


Figure 22: Cumulative number of initially single stars which experience fly-bys in the first 10 Myr with the minimum closest distance of these fly-bys for different values of the initial ratio of the mass of the gas to the mass of the stars $\alpha$ : 1, 3 and 9. The number of stars is the average from the 20 realizations ran for $\alpha = 1$ and 3 and the 10 realizations ran for $\alpha = 9$.

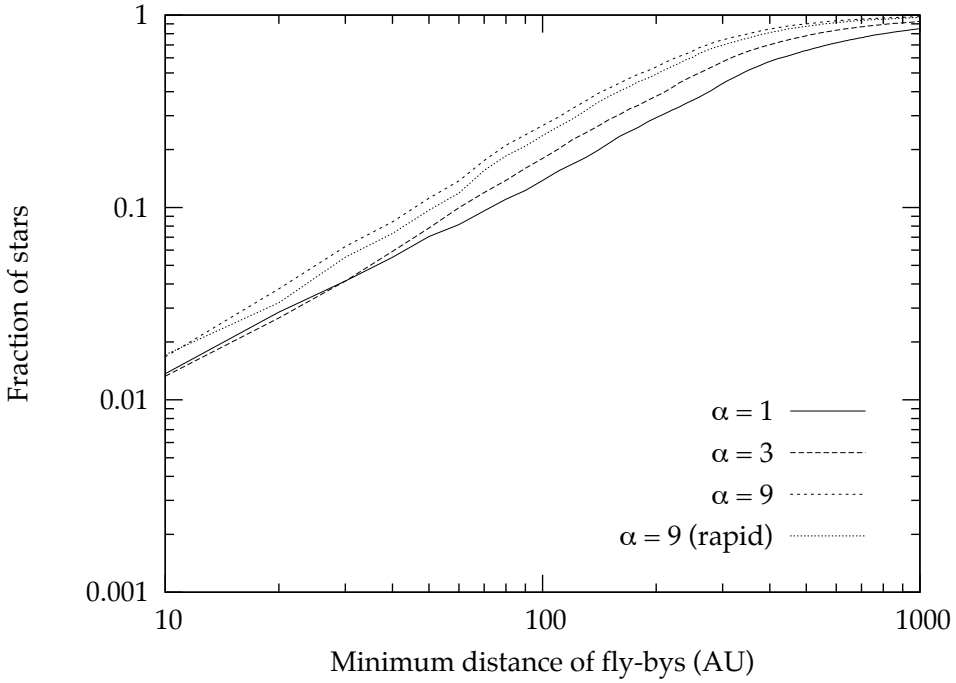


Figure 23: Fraction of initially single stars which experience fly-bys in the first 10 Myr with the minimum closest distance of these fly-bys for different values of the initial ratio of the mass of the gas to the mass of the stars $\alpha$ : 1, 3 and 9. The fraction of stars is the average from the 20 realizations ran for $\alpha = 1$ and 3 and the 10 realizations ran for $\alpha = 9$.

### 5.2.3 Binaries properties

The exchange encounters are now considered. As for fly-bys, the embedded clusters evolution affects their rate. The FORTRAN programs that I wrote to study this effect are similar to those used for fly-bys.

I figure 24, I plot the evolution of the number of exchange encounters experienced by initially single stars in the first 10 Myr with time for different values of $\alpha$. One can see that the rate of exchange encounters is lower for greater $\alpha$. It can be explained as follows. Due to the higher gravitational potential, the velocity dispersion is higher in the clusters with larger $\alpha$. Hence, binaries are more likely to be broken up due to a fly-by according to equation 23. In other words, binaries are softer in clusters with large $\alpha$.

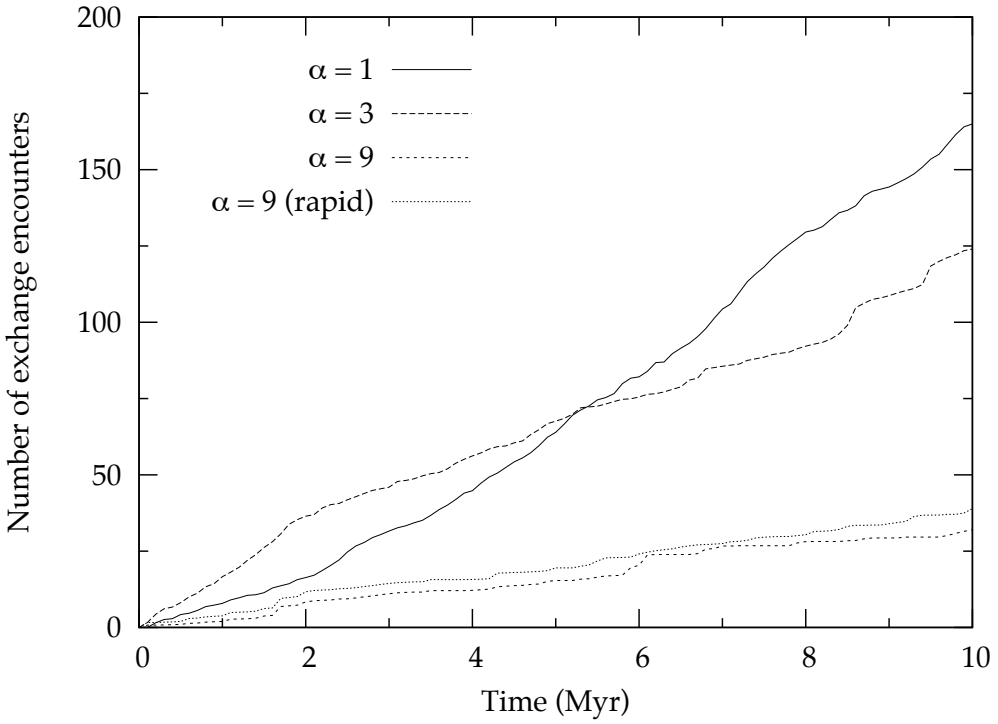


Figure 24: Evolution of the number of exchange encounters experienced by initially single stars in the first 10 Myr with time for different values of the initial ratio of the mass of the gas to the mass of the stars $\alpha$ : 1, 3 and 9. The fraction of stars is the average from the 20 realizations ran for $\alpha = 1$ and 3 and the 10 realizations ran for $\alpha = 9$.

The number and fraction of initially single stars which experience at least one exchange encounter during the first 10 Myr are shown in table 3 for different values of $\alpha$. One can notice that they are low for all $\alpha$ (less than 7 %). Given the large fraction (77 %) of binaries involving single stars in which Kozai mechanism occurs, these exchange encounters can however account for a significant number of perturbed planetary systems.

| Mass ratio | Number of stars which exchange in a binary | Fraction of stars which exchange in a binary |
|---|---|---|
| 1 | 31 | 0.07 |
| 3 | 19 | 0.04 |
| 9 | 8 | 0.02 |
| 9 (rapid) | 7 | 0.02 |

Table 3: Number and fraction of initially single stars which experience at least one exchange encounter during the first 10 Myr for different values of the initial ratio of the mass of the gas to the mass of the stars $\alpha$ : 1, 3 and 9. The number and fraction of stars are the average values from the 20 realizations ran for $\alpha = 1$ and 3 and the 10 realizations ran for $\alpha = 9$.

### 5.2.4 Impact on planetary systems

As for dry clusters, it is interesting to evaluate the effect of encounters on planetary systems. To do so, Venn diagrams are built, showing the encounter histories in the first 10 Myr of all the stars which are initially single. The categories of these diagrams are the same as for dry clusters : the upper circle contains the percentage of stars which are single at the end of the first 10 Myr (S), the lower left circle the percentage of stars which experience an exchange encounter in a binary in the first 10 Myr (B) and the lower right circle the percentage of the stars which have a close encounter during the first 10 Myr (F). The evolution of the number of singletons is also studied during the first 10 Myr. The FORTRAN programs written are similar to those used for dry clusters.

Venn diagrams are shown in figure 25 for $\alpha = 1$, 3 and 9 and $\alpha = 9$ with a rapid gas removal. As predicted in the previous section, the percentage of initially single stars which experience a fly-by in the first 10 Myr (FS) increases when $\alpha$ increases : 78.4 % for $\alpha = 1$ and 96.3 % for $\alpha = 9$. Hence the percentage of singletons at the end of the first 10 Myr is lower for higher $\alpha$ : 14.9 % for $\alpha = 1$ and 2.0 % for $\alpha = 9$. However, the percentage of initially single stars which experience an exchange encounter in this period (FSB and FB) decreases when $\alpha$ is larger : 1.1 % and 0.6 % for $\alpha = 9$ and 5.0 % and 1.7 % for $\alpha = 9$. However, the large percentage of fly-bys compared to exchange encounters does not mean that the effect on planetary systems of fly-bys are more important than that of exchange encounters. Indeed, the probability for a given fly-by to perturb a planetary system is lower than for an exchange encounter. This effect will be studied in further detail in section 6.1.

The evolution of the number of singletons is given in figure 26 for $\alpha = 1$, 3 and 9 and $\alpha = 9$ with a rapid gas removal. The number of singletons drops more steeply for cluster with higher $\alpha$ because of the higher encounter rate. Moreover, as for dry subvirial clusters, this number appears to reach a constant value at the end of the first 10 Myr meaning that the majority of non-singletons are created in this period.

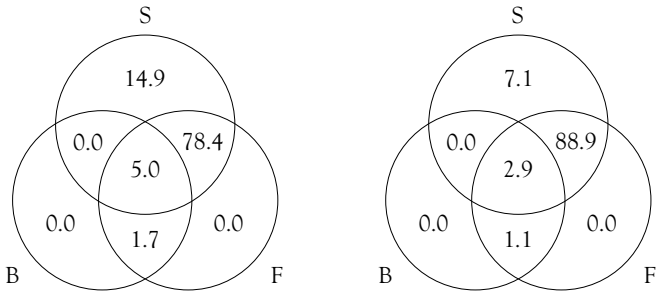


(a) $\alpha = 1$ (b) $\alpha = 3$

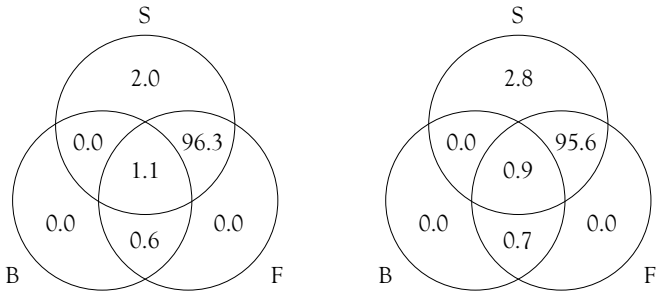


(c) $\alpha = 9$ (d) $\alpha = 9$ (rapid)

Figure 25: Venn diagrams of the stars which are initially single in the cluster at the end of the first 10 Myr for different values of the ratio of the mass of the gas to the mass of the stars : $\alpha = 1$, 3 and 9 and $\alpha = 9$ with a rapid gas removal. The percentages are the averaged values for 20 ($\alpha = 1$, 3) and 10 ($\alpha = 9$) realizations.

| $\alpha$ | 1 | 3 | 9 | 9 (rapid) |
|---|---|---|---|---|
| S | 14.9 ± 2.3 | 7.1 ± 1.2 | 2.0 ± 0.5 | 2.8 ± 0.4 |
| FS | 78.4 ± 2.6 | 88.9 ± 1.3 | 96.3 ± 0.6 | 95.6 ± 0.7 |
| FSB | 5.0 ± 1.2 | 2.9 ± 0.9 | 1.1 ± 0.5 | 0.9 ± 0.4 |
| FB | 1.7 ± 0.6 | 1.1 ± 0.6 | 0.6 ± 0.4 | 0.7 ± 0.3 |
| F | 0.0 ± 0.0 | 0.0 ± 0.0 | 0.0 ± 0.0 | 0.0 ± 0.0 |
| B | 0.0 ± 0.0 | 0.0 ± 0.0 | 0.0 ± 0.0 | 0.0 ± 0.0 |
| SB | 0.0 ± 0.0 | 0.0 ± 0.0 | 0.0 ± 0.0 | 0.0 ± 0.0 |

Table 4: Percentage of the stars for each category of the Venn diagram 10 Myr after the beginning of the run for different values of the ratio of the mass of the gas to the mass of the stars : $\alpha = 1$, 3 and 9 and $\alpha = 9$ with a rapid gas removal. The percentages are the averaged values for 20 ($\alpha = 1$, 3) and 10 ($\alpha = 9$) realizations. The error bars are the standard deviations.

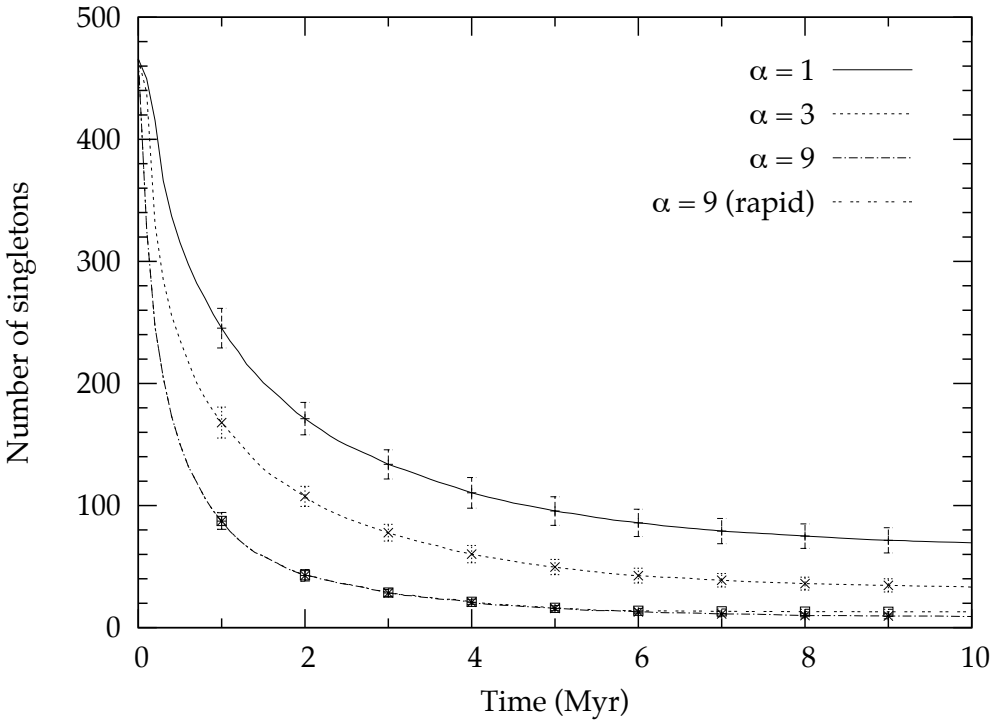


Figure 26: Evolution of the number of singletons with time for different values of the initial ratio of the mass of the gas to the mass of the stars $\alpha$ : 1, 3 and 9. The value of the virial ratio is the average from the 20 realizations ran for $\alpha = 1$ and 3 and the 10 realizations ran for $\alpha = 9$. The error bars are the standard deviations.

# 6 Discussion

## 6.1 Post-encounters evolution of planetary systems

When a host star undergoes a fly-by, one or more of its planets can be ejected. Such ejections can happen immediately but can also occur later after a phase of planet-planet interactions. Hence it is interesting to evaluate the number of planetary systems whose planets are ejected either early or late after a fly-by. Furthermore, this number has to be compared to the number of planetary systems which are affected by the Kozai mechanism during an exchange encounter.

Malmberg et al. (2011) found the probabilities for a planetary system to undergo a planet ejection immediately, in the first 10 Myr, 30 Myr and 100 Myr after a fly-by with a minimum distance $r_{\min} < 100\,\mathrm{AU}$. These probabilities are calculated for three different sorts of planetary systems. The first one is composed of the four gas giants of the solar system (4G) and the second of four Jupiter-mass planets (4J). In the third one, the masses of the gas giants $m_{\mathrm{i}}^{*}$ are defined as

$$m_{\mathrm{i}}^{*} = \sqrt{M_J\, m_{\mathrm{i}}} \tag{41}$$

where $M_J$ is the mass of Jupiter and $m_{\mathrm{i}}$ is the mass of the $\mathrm{i}^{\mathrm{th}}$ gas giant in the normal solar system.

On the other hand, figures 10 and 22 give the number of initially single stars which experience at least one fly-by with a minimum distance of 100 AU in the first 10 Myr for dry and embedded clusters respectively. Hence it is possible to calculate the number of planetary systems which experience an ejection immediately, in the first 10 Myr, 30 Myr and 100 Myr after a fly-by with $r_{\min} < 100\,\mathrm{AU}$. To do so, it is considered that all the stars of the clusters have a mass of 0.6 $M_\odot$. This assumption is reasonable given that 0.6 $M_\odot$ is roughly the mean mass of the stars in the modelled clusters. The results are presented in tables 5, 6 and 7 where the planetary systems are respectively assumed to be all 4G, 4J and GM. The number of initially single stars which experience at least one fly-by with $r_{\min} < 100\,\mathrm{AU}$ is deduced from the N-body simulations performed and can bee seen in figure 10 for dry clusters and in figure 22 for embedded clusters. For these clusters, the number of initially single stars is 466.

When an exchange encounter occurs, the orientation of the orbital plane of the binary with respect to the orbital plane of the planets is expected to be uniformly distributed. Making this assumption, it is possible to compute the percentage of exchange encounters where the inclination between the planets and the companion star is high enough for the Kozai mechanism to happen. Malmberg et al. (2007a) found that 77 % of binaries containing initially single stars, the Kozai mechanism occurs. The number of initially single stars which undergo an exchange encounter in the first 10 Myr is given in table 1 for dry clusters and table 3 for embedded clusters. It allows to compute the number of initially single stars whose planetary system is affected during an exchange encounter. The results are presented in table 8.

For dry clusters, a significant percentage of initially single stars have their planetary system which undergo an ejection of planet either immediately or later after a period of planet-planet interactions (within 100 Myr after the fly-by). For 4G, the values are : 4 % for Q = 0.5 and 12 % for Q = 0.001. One can see that this percentage is similar for initially single stars affected by the Kozai mechanism. For 4G, the values are : 5 % for Q = 0.5 and 10 % for Q = 0.001. For embedded clusters, the percentage of initially single stars which have their planetary system affected by a fly-by is similar. For 4G, the values are : 6 % for $\alpha = 1$ and 12 % for $\alpha = 9$. The percentage of initially single stars affected by the Kozai mechanism is smaller. For 4G, the values are : 5 % for $\alpha = 1$ and 1 % for $\alpha = 9$. For dry and embedded clusters, the effect of exchange encounters on planetary systems is therefore similar to that of fly-bys even if a given star undergoes more fly-bys than exchange encounters. This is due to the large fraction of the exchange encounters which lead to the Kozai mechanism and therefore perturb the planetary systems.

However, the calculated number of stars whose planetary system is affected is only a lower bound. Indeed, it is assumed that the stars undergo only one fly-by with $r_{\min} < 100\,\mathrm{AU}$ each. In reality, the stars are likely to undergo several of these fly-bys. Hence, the combined effect of these fly-bys would induce a higher number of affected planetary systems than calculated in this section with an upper limit given by the number of stars having at least one fly-by with $r_{\min} < 100\,\mathrm{AU}$.

| Virial Ratio | Number of stars with $r_{\min} < 100\,\mathrm{AU}$ | Immediate ejection | $t_{\mathrm{eject}}$ (Myr) 10 | 30 | 100 | No ejection after 100 Myr |
|---|---|---|---|---|---|---|
| 0.5 | 36 | 5 | 7 | 2 | 3 | 19 |
| 0.25 | 67 | 10 | 12 | 4 | 5 | 36 |
| 0.1 | 97 | 15 | 16 | 6 | 8 | 52 |
| 0.01 | 117 | 18 | 20 | 7 | 10 | 62 |
| 0.001 | 120 | 18 | 21 | 7 | 10 | 64 |

| Mass of gas ratio | Number of stars with $r_{\min} < 100\,\mathrm{AU}$ | Immediate ejection | $t_{\mathrm{eject}}$ (Myr) 10 | 30 | 100 | No ejection after 100 Myr |
|---|---|---|---|---|---|---|
| 1 | 64 | 10 | 11 | 4 | 5 | 34 |
| 3 | 84 | 13 | 15 | 5 | 7 | 44 |
| 9 | 124 | 19 | 22 | 7 | 10 | 66 |
| 9 (rapid) | 110 | 16 | 19 | 6 | 9 | 60 |

Table 5: Number of stars whose planetary system 4G undergoes at least one planet ejection immediately, in the first 10, 30 and 100 Myr after a fly-bys with $r_{\min} < 100\,\mathrm{AU}$ for dry clusters (upper table) with different values of the initial virial ratio and for embedded clusters (lower table) with different values of the initial ratio of the mass of the gas to the mass of the stars. For these clusters, the number of initially single stars is 466. The second column contains the number of initially single stars which experience at least one fly-by with $r_{\min} < 100\,\mathrm{AU}$. It is the average value from the realizations ran for each cluster.

| Virial ratio | Number of stars with $r_{\min} < 100\,\mathrm{AU}$ | Immediate ejection | $t_{\mathrm{eject}}$ (Myr) 10 | 30 | 100 | No ejection after 100 Myr |
|---|---|---|---|---|---|---|
| 0.5 | 36 | 6 | 17 | 2 | 2 | 9 |
| 0.25 | 67 | 10 | 32 | 3 | 4 | 18 |
| 0.1 | 97 | 15 | 46 | 4 | 6 | 26 |
| 0.01 | 117 | 18 | 55 | 5 | 8 | 31 |
| 0.001 | 120 | 18 | 57 | 5 | 8 | 32 |

| Mass of gas ratio | Number of stars with $r_{\min} < 100\,\mathrm{AU}$ | Immediate ejection | $t_{\mathrm{eject}}$ (Myr) 10 | 30 | 100 | No ejection after 100 Myr |
|---|---|---|---|---|---|---|
| 1 | 64 | 10 | 30 | 3 | 4 | 17 |
| 3 | 84 | 13 | 40 | 4 | 6 | 21 |
| 9 | 124 | 19 | 58 | 6 | 8 | 33 |
| 9 (rapid) | 110 | 17 | 52 | 5 | 7 | 29 |

Table 6: Number of stars whose planetary system 4J undergoes at least one planet ejection immediately, in the first 10, 30 and 100 Myr after a fly-bys with $r_{\min} < 100\,\mathrm{AU}$ for dry clusters (upper table) with different values of the initial virial ratio and for embedded clusters (lower table) with different values of the initial ratio of the mass of the gas to the mass of the stars. For these clusters, the number of initially single stars is 466. The second column contains the number of initially single stars which experience at least one fly-by with $r_{\min} < 100\,\mathrm{AU}$. It is the average value from the realizations ran for each cluster.

| Virial ratio | Number of stars with $r_{\rm min} < 100\,{\rm AU}$ | Immediate ejection | $t_{\rm eject}$ (Myr) 10 | 30 | 100 | No ejection after 100 Myr |
|---|---|---|---|---|---|---|
| 0.5 | 36 | 5 | 10 | 3 | 2 | 16 |
| 0.25 | 67 | 10 | 19 | 6 | 3 | 29 |
| 0.1 | 97 | 15 | 27 | 8 | 4 | 43 |
| 0.01 | 117 | 18 | 33 | 10 | 5 | 51 |
| 0.001 | 120 | 18 | 34 | 10 | 5 | 53 |

| Mass of gas ratio | Number of stars with $r_{\rm min} < 100\,{\rm AU}$ | Immediate ejection | $t_{\rm eject}$ (Myr) 10 | 30 | 100 | No ejection after 100 Myr |
|---|---|---|---|---|---|---|
| 1 | 64 | 10 | 18 | 5 | 3 | 28 |
| 3 | 84 | 13 | 23 | 7 | 4 | 37 |
| 9 | 124 | 19 | 35 | 10 | 5 | 55 |
| 9 (rapid) | 110 | 17 | 31 | 9 | 5 | 48 |

Table 7: Number of stars whose planetary system GM undergoes at least one planet ejection immediately, in the first 10, 30 and 100 Myr after a fly-bys with $r_{\rm min} < 100\,{\rm AU}$ for dry clusters (upper table) with different values of the initial virial ratio and for embedded clusters (lower table) with different values of the initial ratio of the mass of the gas to the mass of the stars. For these clusters, the number of initially single stars is 466. The second column contains the number of initially single stars which experience at least one fly-by with $r_{\rm min} < 100\,{\rm AU}$. It is the average value from the realizations ran for each cluster.

| Virial ratio | Number of stars which exchange in a binary | Kozai mechanism |
|---|---|---|
| 0.5 | 33 | 25 |
| 0.25 | 43 | 33 |
| 0.1 | 43 | 33 |
| 0.01 | 55 | 42 |
| 0.001 | 62 | 48 |

| Mass of gas ratio | Number of stars which exchange in a binary | Kozai mechanism |
|---|---|---|
| 1 | 31 | 24 |
| 3 | 19 | 15 |
| 9 | 8 | 6 |
| 9 (rapid) | 7 | 5 |

Table 8: Number of initially single stars which undergo at least one exchange encounter (column 2) and number of these stars that are affected by Kozai mechanism for dry clusters (upper table) with different values of the initial virial ratio and for embedded clusters (lower table) with different values of the initial ratio of the mass of the gas to the mass of the stars. For these clusters, the number of initially single stars is 466. The number of stars are is the average value from the realizations ran for each cluster.

## 6.2 Impact of fly-bys on wide planets

The effect of fly-bys on a planetary system depends on how the planets are bound to their host star. Giant planets which form from gas only via the gravitational fragmentation of an unstable protoplanetary disk (without rocky core formation) are likely to be on wide orbits of $\sim$ 100 AU (Boley et al., 2010). These planets are more easily unbound by fly-bys than usual planets because the latter have tighter orbits. For example, Neptune has an orbit of 30 AU. Furthermore, as the number of fly-bys increases with their minimum distance of approach, wide planets are likely to experience more fly-bys than the tighter ones.

To quantify this difference, one can evaluate the number of initially single stars which experience at least one fly-by with a minimum distance of 100 AU and 300 AU. From figures 10 and 22, one can deduce the number of initially single stars which experience at least one fly-by with these minimum distances. The results are presented in table 9. For dry and embedded clusters, one can see that the number of initially single stars which experience at least one fly-by increases by a factor of about 3.

| Virial ratio | Number of stars with $r_{\min} < 100\,\mathrm{AU}$ | Number of stars with $r_{\min} < 300\,\mathrm{AU}$ |
|---|---|---|
| 0.5 | 36 | 106 |
| 0.25 | 67 | 200 |
| 0.1 | 97 | 235 |
| 0.01 | 117 | 262 |
| 0.001 | 120 | 266 |

| Mass ratio | Number of stars with $r_{\min} < 100\,\mathrm{AU}$ | Number of stars with $r_{\min} < 300\,\mathrm{AU}$ |
|---|---|---|
| 1 | 64 | 205 |
| 3 | 84 | 267 |
| 9 | 124 | 346 |
| 9 (rapid) | 110 | 325 |

Table 9: Number of initially single stars which experience at least one fly-by with a minimum distance $r_{\min}$ lower than 100 AU and 300 AU for dry clusters (upper table) with different values of the initial virial ratio and for embedded clusters (lower table) with different values of the initial ratio of the mass of the gas to the mass of the stars. For these clusters, the number of initially single stars is 466. The number of stars are is the average value from the realizations ran for each cluster.

## 6.3 Effect of mass segregation

During the evolution of the cluster, energy is exchanged between stars via two-body encounters. It leads to an equipartition of kinetic energy between stars. Hence the lighter stars have higher velocities than the more massive ones. As a consequence, the latter sink to the centre of the cluster. This process is called mass segregation.

In this section, mass segregation is studied for the dry cluster with Q = 0.5. To bring to light the effect of mass segregation, one has to determine the radial distributions of the stars for different mass ranges and at different times. Therefore I computed this distribution for three different mass ranges (0.8 $M_\odot$ - 1.25 $M_\odot$ and 1.25 $M_\odot$ - 1.75 $M_\odot$, 1.75 $M_\odot$ - 2.5 $M_\odot$) initially and at the end of the first 10 Myr. The NBODY6 code produce a output file containing the masses of the stars at different times. I wrote FORTRAN programs to calculate the distributions from this file. Furthermore, the effect of mass segregation on the encounter histories of the stars is studied. To do so, Venn diagrams are built for different mass ranges where the categories are the same as previously. To produce them, I modified the FORTRAN programs used to obtain the previous diagrams in order to take only into account the stars whose masses are in the three studied ranges. Then I calculated the average from the 25 realizations.

Radial distributions of stars are shown in figures 27 and 28 initially and at the end of the first 10 Myr and for three mass ranges : 0.8 $M_\odot$ - 1.25 $M_\odot$, 1.25 $M_\odot$ - 1.75 $M_\odot$, 1.75 $M_\odot$ - 2.5 $M_\odot$. These results are obtained for an initial virial ratio of 0.5. On can see the effect of mass segregation. The initial radial distributions are similar for the three

mass ranges . However, the more massive stars are further to the centre of the cluster than the lighter ones at the end of the first 10 Myr.

Venn diagrams are presented in figure 29 for the three different mass ranges. The results are summarized in table 10. The number of initially single stars which experience a fly-by (FS) is higher for more massive stars than for lighter ones : it varies from 51.3 % to 56.4 % for the two extreme mass ranges. The same trend can be seen for exchange encounters (FSB and FB) which varies from 6.6 % and 3.7 % to 18.4 % and 11.5 %. The more massive stars are closer to the centre of the cluster which is denser than its outskirts. Hence, they experience more fly-bys and exchange encounters than lighter ones.

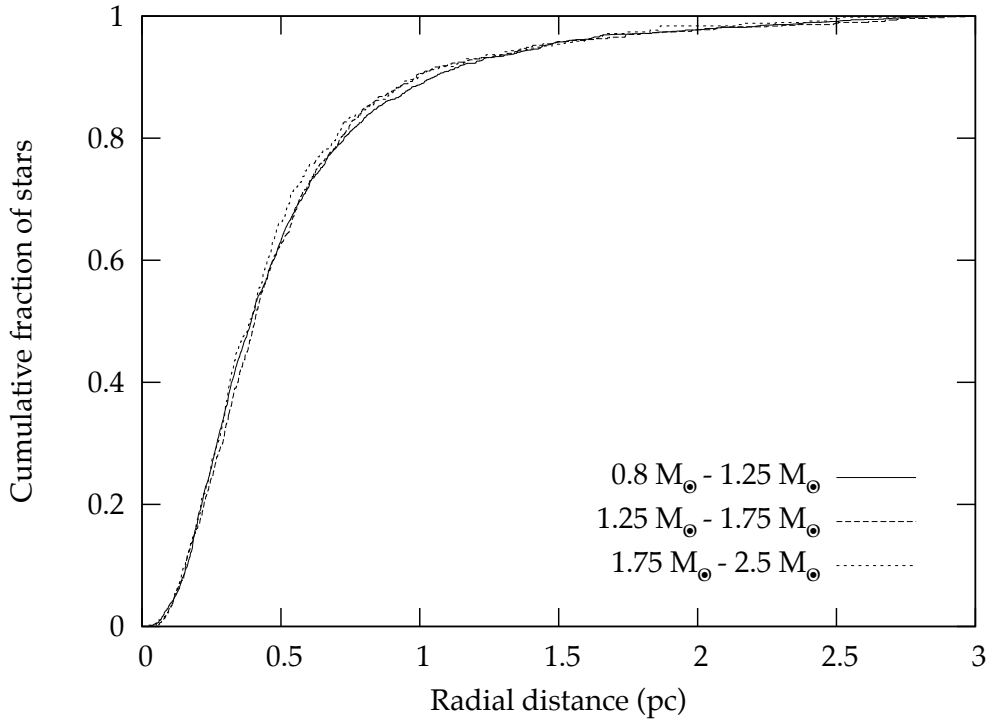


Figure 27: Initial radial distribution of stars for an initial virial ratio of 0.5 and for three mass ranges : 0.8 $M_\odot$ - 1.25 $M_\odot$, 1.25 $M_\odot$ - 1.75 $M_\odot$, 1.75 $M_\odot$ - 2.5 $M_\odot$.

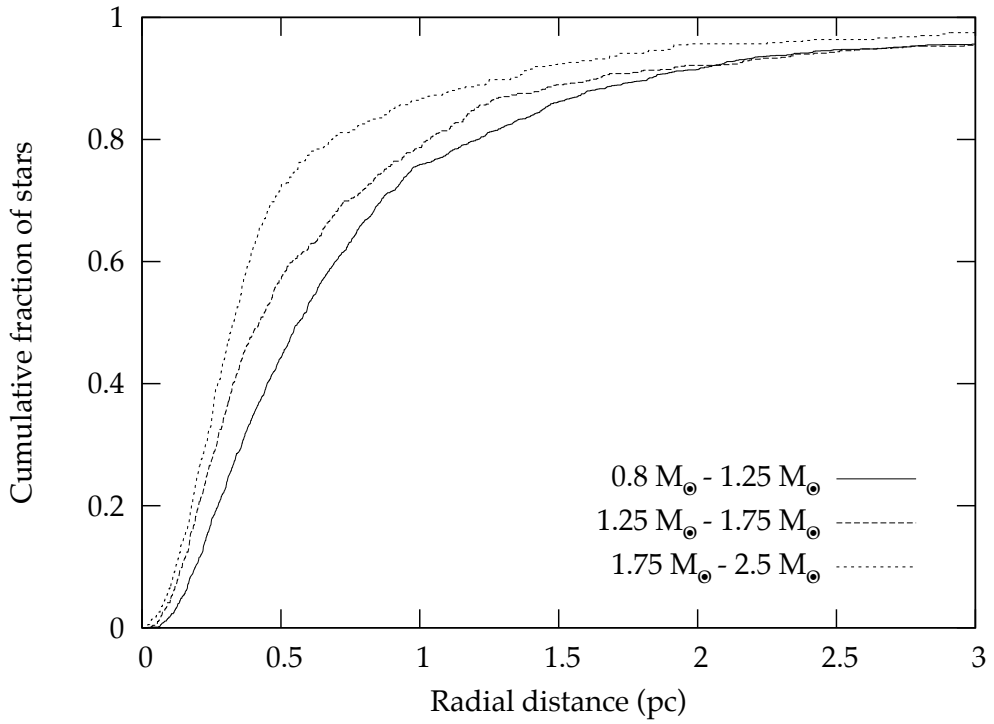


Figure 28: Radial distribution of stars at the end of the first 10 Myr for an initial virial ratio of 0.5 and for three mass ranges : 0.8 $M_\odot$ - 1.25 $M_\odot$, 1.25 $M_\odot$ - 1.75 $M_\odot$, 1.75 $M_\odot$ - 2.5 $M_\odot$.

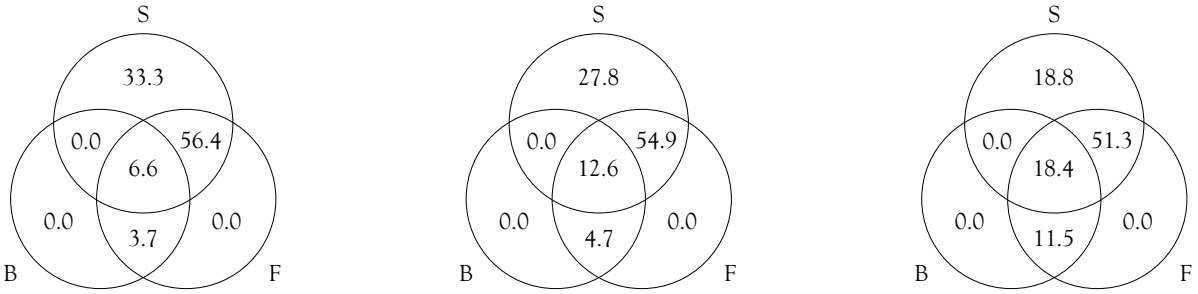


(a) 0.8 $M_\odot$ - 1.25 $M_\odot$ (b) 1.25 $M_\odot$ - 1.75 $M_\odot$ (c) 1.75 $M_\odot$ - 2.5 $M_\odot$

Figure 29: Venn diagram of the stars which are initially single for different mass ranges. The number in each categories represent the percentage of stars in this category at the end of the first 10 Myr averaged over the 25 realizations.

| Mass range ($M_\odot$) | 0.8 - 1.25 | 1.25 - 1.75 | 1.75 - 2.5 |
|---|---|---|---|
| S | 33.3 ± 6.0 | 27.8 ± 11.0 | 18.8 ± 9.5 |
| FS | 56.4 ± 6.0 | 54.9 ± 10.5 | 51.3 ± 10.0 |
| FSB | 6.6 ± 3.7 | 12.6 ± 7.4 | 18.4 ± 12.2 |
| FB | 3.7 ± 2.0 | 4.7 ± 6.8 | 11.5 ± 7.7 |
| F | 0.0 ± 0.0 | 0.0 ± 0.0 | 0.0 ± 0.0 |
| B | 0.0 ± 0.0 | 0.0 ± 0.0 | 0.0 ± 0.0 |
| SB | 0.0 ± 0.0 | 0.0 ± 0.0 | 0.0 ± 0.0 |

Table 10: Percentage of the stars for each category of the Venn diagram 10 Myr after the beginning of the run for different mass ranges. The percentages are the averaged values for the 25 realizations. The error bars are the standard deviations.

# 7 Conclusion

In the previous study, N-body simulations were performed to model dry and embedded young stellar clusters with several initial conditions. These simulations allowed to bring to light the main features of these clusters' evolution. It was seen that all of them shrink in the first 1 Myr of their lives. Furthermore, they are still relatively dense in the next 10 Myr.

The evolution of these clusters turned out to affect the encounter properties in different ways for dry and embedded clusters. It was seen that the rate of fly-bys is enhanced in both cases. However, the number of these fly-bys increases more rapidly with their minimum distance for embedded clusters than for dry ones. Indeed, a fraction of these fly-bys is not dominated by gravitational focussing in embedded clusters. The effect on exchange encounters is also different. Their number is lower in embedded clusters because binaries are more likely to be broken up.

Due to the high rate of fly-bys with a minimum distance of approach $r_{\min} < 1000\,\mathrm{AU}$, the number of singletons is low in these clusters at the end of the first 10 Myr : between 10 % and 20 % for dry clusters and between 5 % and 15 % for embedded ones. Moreover, it was shown that the majority of non-singletons are produced in the first 10 Myr.

The number of stars whose planetary system is affected by close fly-bys (with a minimum distance of approach $r_{\min} < 100\,\mathrm{AU}$) or exchange encounters was also evaluated. Assuming that all the stars in the cluster host the four gas giants of the solar system, it was seen that the number of planetary systems affected ranges in dry clusters from 15 % for Q = 0.25 to 25 % for Q = 0.001 and in embedded clusters from 10 % for $\alpha = 1$ to 15 % for $\alpha = 9$. Moreover, the impact of fly-bys and exchange encounters on these systems are approximately of equal importance. The impact of fly-bys on wide planets was also determined. Assuming that all the stars in the cluster host a wide planet, it was shown that between 45 % and 70 % of these planets are ejected in dry and embedded clusters.

# References

S. J. Aarseth. From NBODY1 to NBODY6: The Growth of an Industry. *PASP*, 111: 1333–1346, Nov. 1999. doi: 10.1086/316455. 12

S. J. Aarseth. *Gravitational N-Body Simulations*. Nov. 2003. 15

P. J. Armitage. *Astrophysics of Planet Formation*. 2010. 10

J. Binney and S. Tremaine. *Galactic dynamics*. 1987. 11, 15

C. M. Boily and P. Kroupa. The impact of mass loss on star cluster formation - I. Analytical results. *MNRAS*, 338:665–672, Jan. 2003. doi: 10.1046/j.1365-8711.2003.06076.x. 9

A. C. Boley, T. Hayfield, L. Mayer, and R. H. Durisen. Clumps in the outer disk by disk instability: Why they are initially gas giants and the legacy of disruption. *Icarus*, 207:509–516, June 2010. doi: 10.1016/j.icarus.2010.01.015. 43

A. Duquennoy and M. Mayor. Multiplicity among solar-type stars in the solar neighbourhood. II - Distribution of the orbital elements in an unbiased sample. *A&A*, 248: 485–524, Aug. 1991. 15

S. P. Goodwin. Residual gas expulsion from young globular clusters. *MNRAS*, 284: 785–802, Feb. 1997. 7

S. P. Goodwin and N. Bastian. Gas expulsion and the destruction of massive young clusters. *MNRAS*, 373:752–758, Dec. 2006. doi: 10.1111/j.1365-2966.2006.11078.x. 8

D. Heggie and P. Hut. *The Gravitational Million-Body Problem: A Multidisciplinary Approach to Star Cluster Dynamics*. Feb. 2003. 13

J. G. Hills. The effect of mass loss on the dynamical evolution of a stellar system - Analytic approximations. *ApJ*, 235:986–991, Feb. 1980. doi: 10.1086/157703. 9

J. R. Hurley, O. R. Pols, and C. A. Tout. Comprehensive analytic formulae for stellar evolution as a function of mass and metallicity. *MNRAS*, 315:543–569, July 2000. doi: 10.1046/j.1365-8711.2000.03426.x. 15

Y. Kozai. Secular perturbations of asteroids with high inclination and eccentricity. *AJ*, 67:591–+, Nov. 1962. doi: 10.1086/108790. 12

P. Kroupa, C. A. Tout, and G. Gilmore. The distribution of low-mass stars in the Galactic disc. *MNRAS*, 262:545–587, June 1993. 13

C. J. Lada and E. A. Lada. Embedded Clusters in Molecular Clouds. *ARA&A*, 41: 57–115, 2003. doi: 10.1146/annurev.astro.41.011802.094844. 6

D. Malmberg, M. B. Davies, and J. E. Chambers. The instability of planetary systems in binaries: how the Kozai mechanism leads to strong planet-planet interactions. *MNRAS*, 377:L1–L4, Apr. 2007a. doi: 10.1111/j.1745-3933.2007.00291.x. 12, 24, 39

D. Malmberg, F. de Angeli, M. B. Davies, R. P. Church, D. Mackey, and M. I. Wilkinson. Close encounters in young stellar clusters: implications for planetary systems in the solar neighbourhood. *MNRAS*, 378:1207–1216, July 2007b. doi: 10.1111/j.1365-2966.2007.11885.x. 11, 12, 17, 19

D. Malmberg, M. B. Davies, and D. C. Heggie. The effects of fly-bys on planetary systems. *MNRAS*, 411:859–877, Feb. 2011. doi: 10.1111/j.1365-2966.2010.17730.x. 38

M. Miyamoto and R. Nagai. Three-dimensional models for the distribution of mass in galaxies. *PASJ*, 27:533–543, 1975. 16

H. C. Plummer. On the problem of distribution in globular star clusters. *MNRAS*, 71: 460–470, Mar. 1911. 12